TRIBHUVAN UNIVERSITY

INSTITUTE OF ENGINEERING

PULCHOWK CAMPUS

EXPERIMENTAL INVESTIGATION OF HEAT TRANSFER PERFORMANCE OF VEHICLE RADIATOR USING AL2O3 NANOFLUID AS COOLANT

SUBMITTED BY:

AANCHAL GUPTA (075BME001)

PUSKAR CHHETRI (075BME032)

SAKSHAM SUBEDI (075BME037)

A REPORT ON

SUBMITTED TO THE DEPARTMENT OF MECHANICAL AND AEROSPACE ENGINEERING IN

PARTIAL FULFILLMENT OF THE REQIREMENT FOR BACHELOR DEGREE IN MECHANICAL ENGINEERING

DEPARTMENT OF MECHANICAL AND AEROSPACE ENGINEERING

PULCHOWK CAMPUS

MARCH, 2023

COPYRIGHT

ABSTRACT

Engine cooling system in I.C. Engine is the mechanism in which excess heat generated by the engine is absorbed by the coolant material. The coolant of an internal combustion engine plays a vital role in the performance of the engine. This topic is currently an active area of research in the field of nanotechnology. This study aimed to investigate the impact of Al_2O_3 nanoparticles of varying concentrations in the radiator of TATA Tiago XZ^+under idle conditions. The Al_2O_3 nano-fluid was prepared via a two-step approach and characterized using UV-Vis spectroscopy. The results indicate an increase in heat transfer rate, thermal conductivity, and overall heat transfer coefficient. These findings suggest that the addition of Al_2O_3 nanoparticles in the radiator coolant can enhance the cooling efficiency of the vehicle.

ACKNOWLEDGEMENT

We would like to express our sincere gratitude to the Department of Mechanical and Aerospace Engineering, Pulchowk Campus, Lalitpur for providing us with the opportunity to conduct this project and get experimental study of the related topic of curriculum.

We would like to express our deepest gratitude to Surya Prasad Adhikari, Ph.D for his utmost support and supervision in our project. The continuous support we got from him has been inspiring us from the beginning and opening us opportunities to move forward. Without his guidance, the project would not have been possible.

We would also like to thank Er. Deepesh Poudel and SIPRADI Trading Private Limited for providing us with required resources to conduct dimensional study and to further conduct tests on cooling system of engine through vehicle radiator. We would also like to thank the co-operation of training committee of company.

We appreciate the co-operation and efforts made by the Department of Applied Sciences and Chemical Engineering for providing us with research lab and nanolab facilities. We would like to thank Mr. Manoj Gyawali for his support for the UV-Vis spectrometer-based characterization of nanoparticles and for band gap calculation.

Thank you all.

TABLE OF CONTENTS

COPYRIGHT ii

ABSTRACT iii

ACKNOWLEDGEMENT iv

LIST OF FIGURES viii

LIST OF TABLES x

LIST OF ABBREVIATIONS xi

CHAPTER 1 INTRODUCTION 13

1.1 BACKGROUND 13

1.2 PROBLEM STATEMENT 15

1.3 Rationale of work 16

1.4 OBJECTIVES 16

1.4.1 Main Objective 16

1.4.2 Specific Objective 16

CHAPTER 2. LITERATURE REVIEW 17

2.1 Heat Exchange Process 17

2.2 History of Car cooling system 18

2.3 History of antifreeze and coolant 19

2.4 Heat Exchanger 20

2.5 Cooling System and Antifreeze 23

2.6 Nanoparticles 26

2.6.1 Types of nanomaterials 27

2.7 Synthesis of nanoparticles: 27

2.8 Synthesis of nanofluid: 28

2.8.1 Two-step approach: 28

2.8.2 One step approach: 31
2.8.3 Other methods: 31
2.9 Experimental analysis: 32
2.10 Characterization of Nanoparticle 33
2.11 Nanofluids as coolant 37
CHAPTER 3 METHODOLOGY 43
3.1 Selection of nanoparticle 44
3.2 Synthesis of Nanoparticle 44
3.3 Characterization of Nanoparticle 50
3.3.1 UV-Visible Nanoparticle analysis 50
3.4 Synthesis of nanofluid: 57
3.5 Experimental Setup: 60
3.5.1 Calculation of thermal properties of base fluid 63
3.5.2 Calculation of thermal properties of Nanofluid fluid: 65
3.5.3 Experimental data analysis: 67
3.5.4 Observation and calculation: 70
CHAPTER 4 RESULT AND DISCUSSION 80
4.1 Effect of Using Nanofluid on Outlet temperature of the Coolant 80
4.2 Effect of Using Nanofluid on Heat Transfer rate of coolant 81
4.3 Effect of Using Nanofluid on Heat Balance Average 82
4.4 Effect of Using Nanofluid on Overall Heat Transfer Coefficient 83
4.5 Effect of Using nanofluid on thermal conductivity applying Maxwell Eucken Equation 84
4.6 Effect of addition of nanoparticle on Viscosity 85
CHAPTER 5 CONCLUSION AND LIMITATION 87

5.1 CONCLUSION 87
5.2 LIMITATION 87
REFERENCES 88
APPENDIX A: UV-Vis spectrophotometer data 96

LIST OF FIGURES

Figure 1 Radiator 21
Figure 2 Freezing and boiling points of water/EG vs. concentration of EG..... 25
Figure 3 Types of sonication instruments bath type (left) and probe sonicator(right) 30
Figure 4 Band gap diagram showing band gaps for conductors, semiconductors and insulators 35
Figure 5 Representative diagram of XRD technique 36
Figure 6 Schematic diagram of FTIR spectrophotometer..... 37
Figure 7 Flow chat of methodology..... 43
Figure 8 Flow chart of nanoparticles synthesis..... 46
Figure 9 300ml Ethanol and 13.34gm Alumunium Chloride 47
Figure 10 Magnetic Stirring of Ethanolic Solution of Alumunium Chloride..... 48
Figure 11 Formation of Gel after drying..... 49
Figure 12 Nanoparticles..... 49
Figure 13 Schematic Diagram for working principle of the UV- Vis Spectrophotometer51
Figure 14 Sample placed on BaSO4 Powder..... 53
Figure 15 Flowchart of the UV test 54
Figure 16:Diffuse reflectance spectra 55
Figure 17 $(hv - hvF(R\infty))2$ curve of $Al2O3$ nanoparticle 57
Figure 18 synthesis of nanofluid of different concentration..... 59
Figure 19 Synthesis of nanofluid using magnetic stirrer 59
Figure 20 TATA Tiago XZ +..... 60
Figure 21 Schematic Diagram of Experimental Setup 61
Figure 22 Data recording at PC 62
Figure 23 3-D Modeling of radiator..... 69
Figure 24 Temperature graph for different concentration of nanoparticle 80
Figure 25 Effect of concentration of nanofluids on the outlet temperature..... 80
Figure 26 Effect of concentration of nanofluids on heat transfer rate of coolant..... 81
Figure 27 Effect of concentration of nanofluids on heat balance average..... 82
Figure 28 Effect of Using Nanofluid on Overall Heat Transfer Coefficient..... 83
Figure 29 Effect of using nanofluid on thermal conductivity..... 84

Figure 30 Effect of addition of nanoparticle on Viscosity..... 86

LIST OF TABLES

Table 1 Analytical Condition 55
Table 2 Nanoparticles properties 65
Table 3 Observation table 70

LIST OF ABBREVIATIONS

EG	Ethylene Glycol
ρ_{nf}	Density of nano-fluid
ρ_C	Coolant density
ρ_p	Density of nano-particles
μ_c	Coolant Viscosity
μ_{nf}	Viscosity of nano-fluid
μ_p	Viscosity of nano-particles
Cp_c	Specific heat capacity of coolant
C_{nf}	Specific heat capacity of nano-fluid
C_p	Specific heat capacity of nano-particles
k_c	Thermal conductivity of coolant
k_{nf}	Thermal conductivity of nano-fluid
k_p	Thermal conductivity of nano-particles
Φ	Volume concentration
Cp_a	Specific heat capacity of air
Q_a	Heat transfer rate of air
Q_c	Heat transfer rate of coolant
U	Overall heat transfer coefficient
m_a	mass flow rate of air
m_c	mass flow rate of coolant
Ta_i	Inlet temperature of air
Ta_o	Oulet temperature of air
Tc_i	Inlet temperature of coolant
Tc_o	Outlet temperature of coolant
ΦEG	Volume concentration of Ethylene Glycol
ΦW	Volume concentration of water

h	Planck’s constant,
v	Frequency of vibration,
α	Absorption coefficient,
Eg	Band gap,
A	Proportional constant
M_{EG}	Molecular weight of Ethylene Glycol
M_W	Molecular weight of water

CHAPTER 1 INTRODUCTION

The engine cooling system in I.C. Engine is the mechanism or process in which the excess heat generated by the engine is absorbed by the coolant material thus reducing the temperature of the engine. The petroleum fuel-powered engine generates heat during its process as the fuel is burnt inside the combustion chamber. The generated heat during this process is the excess heat that could not be transformed\ into useful energy and is either radiated outside the cylinder or conducted through the cylinder walls. The engine has a favorable temperature range to give maximum efficiency for its operation and will underperform if overheated or if the coolant does not perform too well. Thus, the cooling system of an internal combustion engine plays a vital role in the overall performance of the engine.

The cooling process is carried out by the flow of coolant in a given loop inside the engine chamber of the vehicle. The heat generated is absorbed by the relatively cold coolant and the heat is released into the air through the radiator of the engine. The process is generally of two types: Air cooling system and water-cooling system which are named in accordance with the type of coolant used. The water-cooled engine generally uses either Ethylene glycol or Propylene Glycol as a certain amount mixed with water (Mutuku, 2016). The major reason for using this organic compound is due to the high specific heat capacity property it gives when mixed with water.

The major application of any coolant used in the cooling system is to absorb the maximum amount of heat generated during the process and higher specific heat capacity is one of the vital properties of the coolant fluid. The parameters such as heat transfer coefficient, the velocity of coolant, the mass flow rate of coolant, density, specific heat capacity, and others play a crucial role while cooling the excessive heat produced by the engine during its working.

1.1 BACKGROUND

In the early days, when the internal combustion engine has just begun to be manufactured, a proper cooling system was not given them. As the engines were mostly uncovered and the materials used were not properly insulated, they were supposed to be cooled by the

flowing air, which was an unscientific way to solve the heating problem but as it was the first of its kind, it was the best technology available at that time. With time, the requirement for a cooling system was felt by the developers, and the air-cooling system was installed first by the company Mercedes. Wilhelm Maybach designed an air-cooled system using a honeycomb radiator for the 35hp engine of Mercedes which was a great breakthrough for engine cooling systems (RUIAN SHERROCK, 2021).

The air-cooling system was not enough and a change was required in the automobile manufacturing process. A major revolution in the automobile industry was brought about by the introduction of a mixture of Ethylene Glycol with water which could be used as a coolant in the engine due to its favorable properties like high specific heat capacity and heat transfer coefficient. The system contained chambers for coolant flow around the engine known as water jackets from which the coolant flows in a loop. The coolant installed in the engine absorbs heat from the heated regions of the engine and then releases a certain amount of extracted heat to the radiator which has the sole purpose of cooling the coolant and sending it back to the coolant tank.

After a few years of research in this field, a new coolant with similar properties and similar composition was introduced, Propylene Glycol is less toxic than Ethylene Glycol but it lacked heat transfer ability and is less used in automobiles. Both of these compounds were used as coolants by creating a mixture of these compounds by a percentage volume with water. This combination is still widely used in the field of Internal Combustion Engines.

Although this discovery was a breakthrough in the field of engine cooling systems, the heat transfer through the coolant in engines still seems to be a major problem. The overheating of the engine during loaded conditions creates many problems and the inability of coolant seems to be the major reason behind it. The heated engine can destroy other parts of automobiles; the parts of the engine are made to withstand a limited amount of heat and when it is exceeded, they start to deplete causing serious issues with the operation. The conventional coolants have a limited heat conductivity and although the changes such as increased heat exchange area and turbulence have been practiced, the weakness of coolants still prevails. The cooling fins have also been studied but due to limited conductivity

properties, no solid solution has been found in the design or the mechanism of the cooling system.

So, for a better operation of coolant presently in use, a suitable additive can opt for better operation of engine cooling system and longer life of the engine. This option is chosen over the complete replacement of coolant with other compounds because the current coolant is easily available in the market and doing research all over again to discover a better compound is a challenging job. Hence, the addition of nanoparticles as additives in the coolant is the best alternative solution to enhance the performance of the coolant used in the I.C. engine.

Nanoparticles are those particles that range from size 1 to 100nm(nanometer). They are solid particles that can be mixed with a mixture of water and ethylene glycol. A fluid containing suspended nanoparticles is known as nanofluid. The major task of nanofluid is to enhance the performance of the fluid in which the nanoparticles are suspended. Research has shown that the use of nanofluids when used instead of conventional coolant, some oxide nanoparticles exhibit an excellent dispersion property in traditional cooling liquids (Prof. Meshram, Prof. Naik, & Prof. Sonparate, 2015).

1.2 PROBLEM STATEMENT

The conventional coolant does not have enough heat transfer capacity which is causing serious issues in the automobiles. Due to overheating, engine life is decreasing and the vehicles are turning out to be less efficient and the number of problems faced by vehicle owners is increasing rapidly. As the limitation of temperature range for every part of automobile system exists, overheating damages the engine and other parts connected to it. It can cause untimely failure of engine and other parts related to it. The engine getting uncertain breakdowns can cause issues in daily life as well increasing the servicing cost, maintenance cost and also the loss caused due to unavailability of vehicle at times. The heating problem also has direct impact on the fuel consumption and the overall performance of engine output. So, the properties of coolant must be enhanced to solve this overheating issue and increase the general lifetime of engine.

1.3 Rationale of work

The operation of engine in an Internal Combustion Engine involves burning of fuel inside the combustion chamber which results in heating of parts of engine and ultimately both the engine compartment and passenger compartment. Cooling system for the vehicle is a very important part for counterpart of this phenomena. This mechanism is done by the flow of coolant which prevents the vehicle from overheating and also helps in the cold start of engine in extremely cold temperature. The coolant being used currently in the automobile industries is however not enough for this purpose and the thermal properties of coolant can be further improvised to increasing the heat transfer ability of the coolant. For this purpose, an Aluminum based nanoparticle, Al_2O_3 is added to the base fluid (Ethylene Glycol) and analyzed experimentally the difference brought by the addition of nanoparticle in the coolant. The use of nanoparticle has been studied by researchers but not practiced yet by the automobile manufacturers. This experimental analysis aims to increase the overall heat transfer coefficient of the coolant hence increasing the efficiency of the cooling system.

1.4 OBJECTIVES

1.4.1 Main Objective

- To investigate heat transfer performance of vehicle radiator using al2o3 nanofluid as coolant experimentally.

1.4.2 Specific Objective

- To prepare and characterize Aluminum based nanoparticle.
- To synthesize Alumina based nanofluid by using Ethylene Glycol and softened water as base fluid.at different concentration of nanoparticle.
- To compare and analyze the overall heat transfer coefficient of the radiator at different concentration of nanoparticle.
- To study the thermal properties of nanofluid at different concentration of nanoparticles.

CHAPTER 2. LITERATURE REVIEW

Lack of heat dissipation rates in vehicle radiators is a problem brought on by the demand for more powerful engines in smaller hood spaces. Amounting to 33% of the engine's energy produced through combustion is lost as heat from the radiator (Jangra, 2018). Inadequate heat dissipation can cause the engine to overheat, which causes the lubricating fluid to break down, the metal in the engine parts to weaken, and substantial wear between the engine parts.

In a vehicle, combustion occurs inside the engine to provide power. Only a portion of the total power generated is used to actually operate the car; the remainder is lost as heat and exhaust. The engine will overheat, the lubricating fluid will break down in viscosity, the metal on the overheated engine parts will weaken, and stress between the engine parts will cause the engine to wear out more quickly if this extra heat is not eliminated. To get rid of this excessive heat, a cooling system is employed. Radiator, water pump, cooling fan, radiator pressure cap, and thermostat make up the majority of car cooling systems (Types of Cooling System in Car Engine: Components & Function, 2021).

The radiator is the system's most noticeable feature among these parts since it transmits heat. Heat builds up in the coolant as it passes through the cylinder block of the engine. The thermostat in the car opens a valve, forcing the coolant to flow through the radiator, once the coolant temperature rises above a predetermined threshold (Smith & Holroyd, 2013). Heat is delivered to the air through conduction and convection through the radiator's fins and tube walls as the coolant circulates through its tubes.

2.1 Heat Exchange Process

An automobile gets heated from different means. The heat generation occurs from engine compartment itself, due to the friction that occurs between the components and also due to the surrounding factors. These things can directly or indirectly increase the temperature of the vehicle or generate heat above tolerable level for a vehicle. The heat must be taken away from the working components of vehicle else the efficiency can drop. The process of heat absorption from the hotter parts and releasing it to the surrounding is done by the coolant used in the vehicle (Yang, et al., 2023).

The coolant acts as the working fluid as it absorbs the heat from the heated parts of engine and passenger compartment and releases it to the relatively colder ambient air. The coolant is flown from the coolant pump to the different heated parts of engine through water jacket or water passages and the heated coolant is sent to the radiator where it loses the heat absorbed to the ambient air by forced convection executed by the cooling fan.

2.2 History of Car cooling system

In the past, heating, ventilating and cooling of parts of automobile (mainly engine) was a sophisticated process. One way to maintain air flow was through the windows of vehicle, but this allowed the surrounding air inside the vehicle that was as cold, hot or dusty as the outside which became a major problem. Thus, in unfavorable conditions, the windows could not be opened and cooling was not possible in those cases.

During cold weather, clay bricks were warmed up on a cast-iron stove as it was easily available and simple to obtain from household. It could be placed on the floor of the vehicle and it radiated heat inside the vehicle until it got cold. Installing a small heater that burned charcoal or coal to warm the passengers was a cultured practice as well.

During hot weather, the driver and passengers would be left with nothing but discomfort due to poor cooling system in the vehicle. Some innovative people attempted to cool the vehicle compartment by keeping a block of ice inside the vehicle. Neither of the solutions was convenient or effective for the vehicle and the passenger which led the automobile manufacturers to develop an automobile conditioning system. The first of it's kind was developed by Karl Benz. Wilhelm Maybach designed the first honeycomb radiator which was patented for the Mercedes 35hp which was successfully tested and installed vehicle with a proper cooling system.

In mid 1900s, vehicle with air conditioning systems were manufactured such as the Cadilacs and Chrysler. In 1948, Automotive Refrigerated Air Conditioning (ARA) was the first company to offer vehicle manufacturers an air-conditioning system in kit form.

In present day, Automobile manufacturers mostly use liquid cooling system in the vehicles to achieve and maintain an efficient and optimized operation temperature range. A vehicle engine generates enough heat to cause thermal stress or even ignite the components. To

limit this damage that can be caused due to overheating, coolant is circulated through pipelines and water jackets in the engine block and cylinder area to take away the excess heat. Coolant plays a significant role by absorbing the heat from the engine and letting it off through the radiator. The heat absorbed is also sometimes used to heat the passenger compartment of the vehicle thus recycling the waste heat within the vehicle (History of Car Cooling System, 2018).

2.3 History of antifreeze and coolant

Antifreeze is a very crucial mixture for machines and engines in extreme surroundings. It carries invaluable worth in cold start of engine. Antifreeze was invented to surpass water's inadequacies as a heat transfer agent. It not only helps engine to start in severely cold environment but also hot climates.

Generally, this substance is produced by mixing softened(distilled) water with base fluid such as mono ethylene glycol or mono propylene glycol. Additionally, specific types of additives are added to the antifreeze to prevent corrosion, rusting whilst giving specific color to the coolant.

The history of antifreeze goes back to the Napoleonic era in Paris. The historical development is as follows:

1856: French chemist Charles-Adolphe Wurtz invented ethylene glycol, a material that had a higher boiling point and lower freezing point compared to water. It had a very low viscosity, making it easier to pump through the lines in engine and the radiator.

Late 1800s, early 20^{th} century: To prevent early automobiles from overheating, methyl and wood alcohols were used. Despite having lower freezing points than water, these industrial solvents were highly corrosive to metal parts and hence were responsible for wear and tear.

Early 1900s: Glycerol was used as antifreeze widely but due to the high costs involved in the manufacturing, it was later replaced by ethylene glycol.

1918: The commercial production of Ethylene glycol began and it was primarily used in explosives.

1926: Use of Ethylene Glycol as automotive antifreeze began, which was later adopted by the military during World War II.

Post-World War II: Ethylene glycol, which took over the market, became the primary chemical antifreeze. Although Propylene glycol and organic acid technology (OAT) exist as substitutes for Ethylene glycol, no other material has overcome the properties shown by Ethylene glycol and it still holds the majority of market.

2007: Ethylene glycol is widely used in automobile coolants, machineries antifreeze and manufacturing of polyester fibers (The Versatile Fluid That Changed The World, 2018).

2.4 Heat Exchanger

A specific kind of heat exchanger is a radiator. The heated coolant that passes through it is intended to impart heat to the air being blasted through it by the fan. Aluminum radiators are the norm in modern vehicles. These radiators are constructed by brazing flattened metal tubes to tiny aluminum fins. From the entrance to the outlet, the coolant travels through several tubes stacked in parallel. The fins transport heat from the tubes and disperse it into the radiator's airflow. A fin known as a turbulator may occasionally be put into the tubes to increase the turbulence of the fluid passing through them. Only the fluid directly touching the tubes would experience direct cooling if the fluid travels through the tubes very smoothly. The temperature difference between the tube and the fluid touching it determines how much heat is transmitted to the tubes from the fluid flowing through them. Therefore, less heat will be transported if the fluid in contact with the tube cools down quickly. All of the fluid inside the tube is used efficiently by generating turbulence inside the tube, which keeps the temperature of the fluid hitting the tubes up so that additional heat can be removed. On each side of radiators is typically a tank with a transmission cooler. The coolant flows in multiple passes in the radiator which decreases the flow rate of coolant inside the pipes and the heat is lost in the surrounding. Higher the temperature of engine operation, the higher will be the temperature of coolant and more heat needs to be released through the radiator fins. Almost every vehicle has radiators in the frontal part so the air directly hit the tubes and increases the efficiency of the cooling process. It is a part of cooling system assembly of vehicle which dumps out the heat from the engine and plays a vital role in the engine economy and efficiency. It is also very important to keep

the engine always in the working temperature range. For this operation, a thermostat valve is also set between the engine water outlet and the radiator water inlet port. Only when the desired temperature is reached, the engine and all other parts and process can function properly (Palani, Irudhayarai, Vigneshwaran, & Selvam, 2016).

The transmission cooler functions similarly to a radiator within a radiator, with the exception that the fluid in the radiator cools the coolant, not the air. The fluid is introduced into the engine block by the pump and travels around the cylinders in the engine through passageways. Then it exits the engine through the cylinder head. Where fluid exits the engine is where the thermostat is positioned. If the thermostat is closed, the tubing surrounding it immediately transfers the fluid back to the pump. If it's wide open, the liquid first passes through the radiator before returning to the pump.

The heating system has its own circuit as well. This circuit sends fluid from the cylinder head back to the pump after passing it via a heater core. There is typically also a separate circuit for cooling the transmission fluid integrated into the radiator on vehicles with automatic transmissions. The Diagram of the Radiator with its component is shown below.

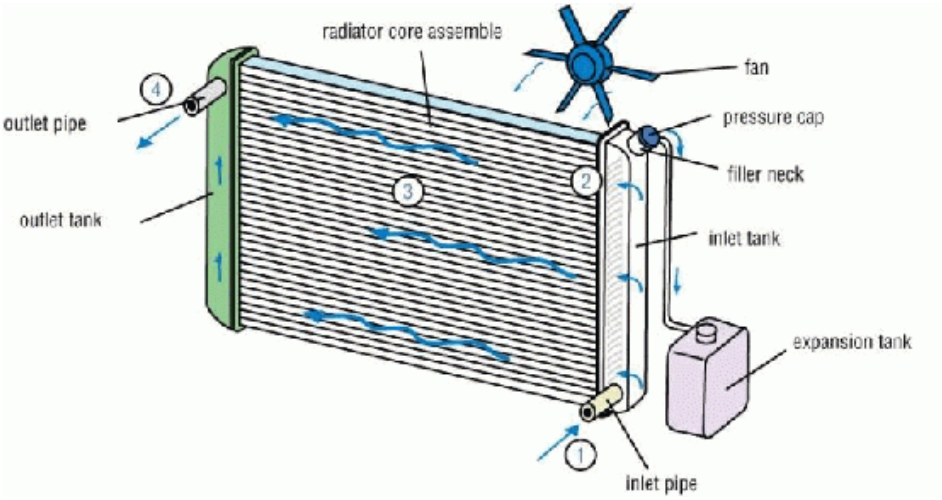

Figure 1 Radiator *(Studentlesson, 2020)*

Automobile radiators typically use a cross-flow heat exchanger and are composed of aluminum. Typically, air and coolant are the two operating fluids (50-50 mix of water and

ethylene glycol). Heat is transmitted from the coolant to the air as it passes through the radiator. The coolant exits the radiator at a lower temperature than it arrived by virtue of the air's ability to take heat from it. 140 kW of heat at a 95 °C input temperature is the standard for heat transmission for modern radiators. The dimensions of the standard radiator are 0.025-0.038 m (1-1.5") in depth, 0.4-0.7 m (16-27") in height, and 0.5-0.6 m (20-23") in width (Pathade, et al., 2017).

The part of the automobile radiator is explained below:

Core

The core of the radiator is the major component that performs its primary purpose. It is a metal cylinder with small metal fins that allow heat from the coolant to be released to the nearby air of the radiator. Radiators are classified according to their cores, such as one-, two-, or three-core radiators.

Pressure Cap

Due to the constant pressure in the radiator, the coolant may be kept significantly hotter beneath without boiling. As a result, the system is significantly more effective. Since the heated coolant eventually rises, the pressure cap's purpose is to drain out the excess heat. If the pressurize cap is malfunctioning, the hot coolant might damage the coolant components.

Outlet and Inlet tank

The radiator's inlet and outlet are where the water flows into and out of it. The radiator head, which is constructed of metal or plastic, is where it is positioned. Hot coolant from the engine passes through the radiator's intake section and out through the other to the engine. The connections are made via the hose.

Cooler

In certain vehicles, the engine and gearbox coolers are the same cooler. To maintain coolant circulation in the transmission system, the fluid travels via a steel pipe. Since heat is also produced by an automatic transmission, this coolant is also cooled inside the radiator. Nevertheless, some engines are built with a transmission radiator that is distinct.

2.5 Cooling System and Antifreeze

The cooling system of a car is the grouping of components and fluids (coolants) that cooperate to keep the engine's temperature at ideal ranges. The system, which is made up of a variety of parts including a water pump, coolant, a thermostat, etc., enables the engine to run smoothly and effectively while safeguarding it from harm. An automobile's engine produces a tremendous quantity of heat when it is operating. Every minute, thousands of carefully controlled explosions occur inside the engine throughout each combustion cycle. The engine would self-destruct if the car kept racing and the heat generated within wasn't released. Therefore, it is essential to simultaneously eliminate the waste heat.

The engine's cooling system is specifically designed to maintain the temperature within acceptable ranges, even though waste heat is also dispersed by the intake of cool air and the outflow of hot exhaust gases. The core components of the cooling system include passageways in the engine block and heads, a pump to circulate the coolant, a thermostat to regulate coolant flow, a radiator to cool the coolant, and a radiator cap to regulate system pressure. The system circulates the liquid coolant through tubes in the engine block and heads to produce the cooling action. The coolant absorbs heat as it passes through and then returns to the radiator to be cooled. After then, the coolant is cycled once again to keep the engine's temperature within acceptable ranges (Idik, YAzid, & Mamat, 2015).

In the automotive sector, engine coolant is frequently used to refer to its main purpose of convective heat transmission. Corrosion inhibitors are also employed in the automobile industry to assist safeguard the cooling systems of cars, which frequently include a variety of metals that are incompatible with electrochemistry (aluminum, cast iron, copper, lead solder, etc.). To address the drawbacks of water as a heat transfer fluid, antifreeze was created. In most engines, freeze plugs are installed in the engine block to safeguard the engine in the event that the cooling system's antifreeze failed or if the outside temperature fell below the antifreeze's freezing point. If the engine coolant becomes too hot, it might boil inside the engine, creating voids (pockets of steam), which could cause the engine to fail catastrophically. Both issues may be solved by using the right engine coolant and a pressurized coolant system. Some antifreeze prevents freezing up to 870 degrees Celsius (Stefl & George, 2000).

An engine cooling system's main function is to reduce metal temperatures to safe levels and remove extra heat created by engine running. Modern engines may generate enough heat energy when travelling at high speeds to melt a 200 lb (91 kg) cast iron engine block in 20 minutes. The engine's internal temperatures are very high even while it's moving at a reasonable speed. It is possible for combustion gas temperatures to reach 4500°F (2482°C). The temperature of lubricated parts, such as pistons, may reach 200°F (93°C) or more over the boiling point of water, and the exhaust valves' heads may be red-hot. Lubrication failure and significant engine damage result when metal temperatures are not controlled by appropriate cooling. This is particularly valid for engines with aluminum heads (Joseph A. Lima and George R. Otterman, 1989).

Methanol

Methanol is a chemical molecule with the molecular formula CH3OH, also known as methyl alcohol, carbonyl, wood alcohol, wood naphtha, or wood spirits. It is the most basic alcohol and is a colorless, flammable, light, volatile liquid with a unique scent that is somewhat sweeter and milder than ethanol (ethyl alcohol). It is a polar liquid that is utilized as an antifreeze, fuel, solvent, and denaturant for ethyl alcohol at room temperature. Although it is not extremely common for equipment, it may be found in fuel additives, deicers, and windshield washer fluid for cars, to mention a few (Knorr, Sanchez, Schirmer, Gazdzicki, & Friedrich, 2019).

Ethylene Glycol

Ethylene glycol, also known by its IUPAC designation of ethane-1, 2-diol, is a common organic molecule used as an antifreeze for automobiles and as a building block for polymers. It is an odorless, colorless, syrupy liquid with a pleasant taste in its purest form. Ethylene glycol, however, is poisonous and can be fatal if consumed. Since ethanol solutions' higher boiling temperatures offered benefits for usage both in the summer and during cold weather, they were advertised as "permanent antifreeze" when they first became commercially accessible in 1926. They are still used today for many other purposes, including cars. Because it is so common, ethylene glycol poisoning has occasionally occurred as a result of ingestion. Because of its toxicity, ethylene glycol-containing coolant shouldn't be disposed of in a method that may cause animals to consume

it ((Hollis, Lovas, Jewell, & Coudert, 2002). Use of ethylene glycol for coolant has become common and this is majorly due to the alteration in the property of water when mixed with Ethylene Glycol. The cooling system of any engines or machines might have been operated by using water as coolant in the past but due to the alteration capacity of Ethylene glycol when added to softened water had changed the scenario as the freezing point and boiling point of water is changed when Ethylene Glycol is added to it.

Percentage of EG in water	Freezing point (°C)	Boiling point (°C)
0	0	100
10	−4	102
20	−7	102
30	−15	104
40	−23	104
50	−34	107
60	−48	110
70	−51	116
80	−45	124
90	−29	140
100	−12	197

Figure 2 Freezing and boiling points of water/EG vs. concentration of EG *(Che Sidik, Mohd Yazid, & Mamamt, 2015)*

Coolants are generally the mixture of Ethylene Glycol with distilled water in an appropriate ratio. The most effective ratio is either given in the label of product or should be studied first to apply. In modern day coolants, it has become necessary to add some performance enhancers in the coolant which are also known as surfactants or coolant additives.

Surfactants

For the coolant to be performing efficiently, it must have special abilities such as anti-corrosive and anti-depository properties. Surfactants are those chemical compounds which are responsible for the decrease in surface tension of fluid in which they are added into.

Different types of surfactants and respective concentration can be added to the fluid according to the study carried on (Furuya & Kinoshita, 2002).

2.6 Nanoparticles

"Nanotechnology" has obtained a great development in the present scenario after its breakthrough since presented by Laureate Richard P. Feyman from his famous lecture from 1959 "There's plenty of room at the bottom" (Feynman, 1960) . The revolutionary ideas and discoveries brought by Nanotechnology include products at various nanoscale levels. Nanoparticles are particulate substances whose dimension of one side is less than 100 nm (nm= 10^{-9}) at the least (Laurent, et al., 2010). The whole idea about nanotechnology is to effectively reduce the size of particle and deliberately providing no losses in comparison to the larger model while conducting any operation. Nanotechnology needs nano-sized parts to assemble together and thereby, they are also recognized as the tiny materials whose size range from 1 to 100 nm (Khan & Khalid Saeed, 2019). It is limited to 1nm because the atomic bond lengths are reached at 0.1nm. The size of particles cannot go to this limit as it is limited due to the bond length between two atoms of same substance.

Nanoparticles naturally exist in the world and are also created from different human activities. The breaking down of heavier stones into sand particles after being in pressure naturally or by human activity is the perfect example of how nanomaterials are formed. As they are microscopic in size, they have versatile field of application generally in medicine, catalyst, engineering and remediation. They occupy lesser area and hence can be used in complex applications without disturbing any other operations being carried out in nearby periphery. Due to their significant property of high surface to volume ratio, small amount of nanoparticles can bring large impact in application by presenting large area of contact (Klein, 2007). The different shapes of nanomaterials include nano cube, nanoclusters, nanospheres, nano reef, nanowires and nanotubes. The information regarding the morphology of different phases, number of phases, crystallographic defects and chemical composition can be obtained from the microstructural characterization (Mayeen, Shaji, Nair, & Kalarikkal, 2018).

A crucial part of study after the synthesis of nanoparticle is the characterization. The obtained material must be tested to confirm that it follows the lawful property and is a

defined nanoparticle. Nanoparticle size-based characterization is complicated by polydispersity of samples. Because of very small size of particles, the molecular weight distribution along length or breadth might not be in a noticeable pattern. However, characterization can be done by multiple methods such as UV testing, XRD, TEM and DLS methods (Jennifer, Marina, Anil, & E, 2007).

2.6.1 Types of nanomaterials

Nanomaterials can be categorized into four types:

1. Inorganic based nanomaterials
2. Carbon-based nanomaterials
3. Organic-based nanomaterials
4. Composite-based nanomaterials

Generally, inorganic nanomaterials consist of metal and metal oxides of nanomaterials. Some of the metal based inorganic nanomaterials are silver (Ag), aluminum (Al), Copper (Cu), Gold (Au), Zinc (Zn), Cadmium (Cd) and Lead (Pb) nanomaterials. Some of the metal-oxide based inorganic nanomaterials are Magnesium Aluminum oxide ($MgAl_2O_4$), Aluminum oxide (Al_2O_3), Copper oxide (CuO), Zinc Oxide (ZnO), Iron Oxide (Fe_3O_4), etc. Graphene, Multiwalled carbon nanotube, carbon fiber, fullerene and activated carbon are some nanomaterials based on Carbon. The Organic based nanomaterials consist of materials derived from organic materials excluding carbon materials, for instance, liposome, micelle, dendrimers and cyclodextrin. The combination of metal-based, metal oxide-based, carbon-based and/or organic-based nanomaterials produce composite nanomaterials which have complicated structures like metal-organic framework (Majhi & Yadav, 2020).

2.7 Synthesis of nanoparticles:

Nanoparticle synthesis is a quickly developing area with wide applications in sectors such as electronics, medicine, and energy. There have been many breakthroughs in nanoparticle synthesis techniques in recent years, including chemical, physical, and biological approaches. To make nanoparticles, metal compounds are reduced or oxidized in a liquid. In recent years, there has been a rise of interest in the application of green chemistry

concepts to nanoparticle production. Nanoparticle synthesis also uses physical methods, including laser ablation, chemical vapor deposition, and spray pyrolysis. These methods involve the use of high temperatures and energy to produce nanoparticles, resulting in controlled size, shape, and composition.

Using a sol-gel approach, a combination of aluminum nitrate and citric acid would be able to synthesis two distinct phases of alumina (Al_2O_3) nanoparticles. The alumina nanoparticles' efficacy as an adsorbent cannot be dependent on their phases, but might be attributed to increasing particle size at higher sintering temperatures (Mohamad, et al., 2019). The Al_2O_3 was synthesized by using the two methods both were the solgel method using Aluminium Chloride, ethanol and ammonia for the 1st method and aluminum nitrate, malic acid and polyvinylpyrrolidone for the 2nd method , both the methods uses heating treatment to produce Al_2O_3 as a powder form (Sahoo, 2015). Cu-Al_2O_3 nanoparticles were prepared by using two chemical routes (Shehata, Fathy, Abdelhameed, & Moustafa, 2009). Al_2O_3 nanoparticles were prepared by using Triton X-l00/n-butylalcohol/ cyclohexane/ water W/O reverse microemulsion (Ke-long, Liang-guo, Su-qin, & Chao-jian, 2007). A pechini process was used to synthesize alpha- aluminum at relatively low temperature where final product was obtained after a dual-stages thermal treatment (Zaki, kabel, & Hassan, 2012).

2.8 Synthesis of nanofluid:

Nanofluids are fluids containing nanoscale particles that exhibit enhanced heat transfer properties and have a wide range of applications in various industries. In recent years, there have been many advances in nanofluid preparation methods, they are two-step approach and one-step approach.

2.8.1 Two-step approach:

The two-step method for making nanofluids includes two distinct processes: nanoparticle synthesis and nanoparticle dispersion in a base fluid. The first stage is to create nanoparticles using different techniques such as chemical precipitation, sol-gel, or laser ablation. The synthesized nanoparticles are disseminated in a base fluid using different techniques such as sonication, stirring, or high-pressure homogenization in the second. A novel two-step technique was used for preparing efficient MgO-DW nanofluid, at room

temperature, without using surfactants and/or organic base fluids (Judran, et al., 2022). Al_2O_3 -cu nanofluid was prepared by two step method and was found that there is a significant enhancement of the thermal conductivity (Suresh, Venkitaraj, Selvakumar, & Chandrasekar, 2011). Al_2O_3 -TiO_2 -water hybrid nanofluid also prepared by two step method and it noticed that the thermal conductivity of Al_2O_3 -TiO_2 -water hybrid nanofluid was discovered to be higher than the thermal conductivity of the base fluid, which is water (Septiadi, Trisnadewi, Putra, & Setyawan, 2018).

2.8.1.1 Solgel method:

The sol-gel method, an industrial process, creates nanoparticles with various chemical compositions by producing a uniform sol from precursors, converting it into a gel, and removing the solvent before drying the remaining gel (Bokov, et al., 2021). CuAlO2 was synthesized using the sol-gel technique and the nitrate-citrate pathway, as well as the solid-state reaction method and it was found that the particle size produced by the nitrate-citrate approach is smaller than the particle size produced by the solid-state reaction process (Ghosh, Popuri, Mahesh, & Chattopadhyay, 2009). ZnO particles have been synthesized by solgel method where the average particle size was found to be 58.3mm (Alwan, et al., 2015). (Ahmed & Abdel-Messih, 2011) used a controlled sol-gel technique to make titania-alumina nanocomposites (x = 0, 10, 20, 40, 60, 80, and 100 wt%Al_2O_3) using simple salts of lower costs as metal chlorides. New precursors, including aluminum nitrate, ethylene glycol (EG), citric acid (CA), and triethanolamine (TEA), were employed as Al3+ source, gel, chelating, and surfactant agents, respectively, to synthesize γ-Al_2O_3 nanoparticles using a modified sol-gel method (Tabesh, Davar, & Loghman-Estarki, 2018).

2.8.1.2 Ultrasonication method:

It is the method of treatment of liquid sample with ultrasonic waves (>20 kHz) which result in agitation. The sound waves being propagated into the liquid medium result in creating compression (high pressure) and rarefaction(low-pressure) regions in alternating cycles. Small vacuum bubbles are created when the liquid is hit by the high intensity sonic wave during rarefaction, which collapse violently during the compression action and forms cavitation resulting in sudden increase of temperature. The rise in temperature can go up to 5000K and pressure up to 1000 bar (Sivakumar, Tang, & Tan, 2014).

This technique is generally utilized to break large particles into smaller fragments or uniform sized particles in the base fluid. This method provides a good control over the characteristics of nanoparticles. The cavitation process initiate desired physical transformation in the specimen which when studied can be useful to obtain the property required for any experiment. This technique also provides control over the particle size distribution and in improvement of the stability of nanoparticles (Yilmaz, Karasulu, & Yilmaz, 2019).

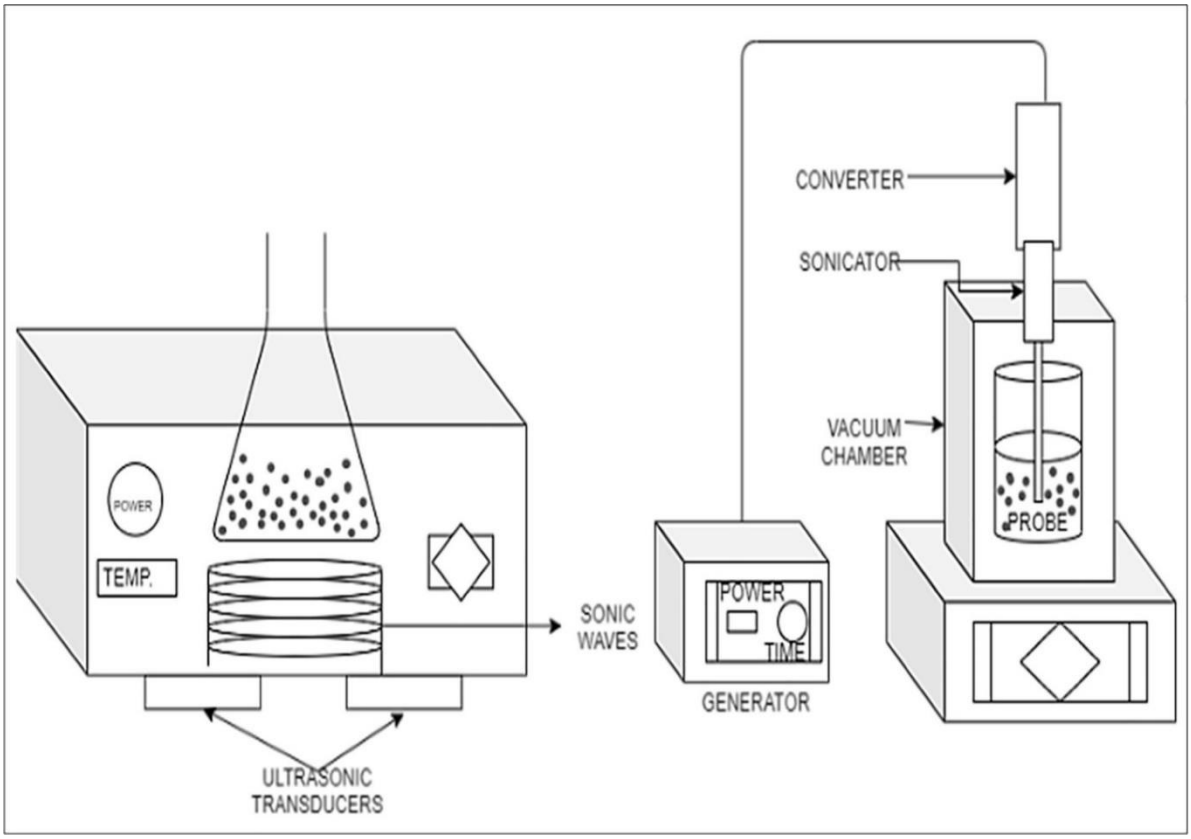

Figure 3 Types of sonication instruments bath type (left) and probe sonicator (right) *(Sandhya, Ramasamy, Sudhakar, Kadirgama, & Harun, 2021)*

2.8.1.3 Magnetic Stirrer:

Magnetic Stirrer is a device used in laboratories for stirring purpose. It operates by the rotating magnetic field being generated by a stationary electromagnet. This device reduces the effort for manual stirring of solution without directly influencing the chemical properties of the solution. It is used for mixing of solution through quick spinning of a

special type of magnet that is immersed inside the liquid which aligns magnetically with the device (Loos, 2015). The strong magnetic field created by the magnetic stirrer creates a high-speed stirring action which is enough to make the mixture homogeneous. However, the purpose of breaking down of the agglomerates might not be efficiently done with this method. This leads to instability and sedimentation of nanofluid. (Bhanvase & Barai, 2021) Continuous stirring can be done to overcome this defect but it can be time consuming and laborious for the experiment. In an experiment conducted by Chaudhari et al., it took almost 10 hours of magnetic stirring for the preparation of Aluminum based nanofluid (Al_2O_3) which could only remain usable for the next 8 hours (Chaudhari, Walke, Wankhede, & Shelke, 2015) .To overcome this defect, the magnetic stirring process can be followed by ultrasonication (Cabaleiro, et al., 2017).

2.8.2 One step approach:

The one-step technique involves preparing and dispersing nanoparticles simultaneously, eliminating drying, storage, and transportation processes, reducing agglomeration, and improving fluid stability, resulting in uniformly dispersed and stably suspended nanoparticles in the base fluid (Rathodiya & Vishnoi, 2017). Physical Vapor Deposition (PVD) technique is used for preparation of stable nanofluid. In this method, direct evaporation and condensation of nanoparticles is done in the base fluid (Ali & Salam, 2020). The main drawback of one step method is that the cost of process is higher than the other methods and the residual reactants are left in the nanofluids which causes the formation of deposits in the vessel or the pipe in which the fluid is flown through reducing the efficiency of operation and can cause damage of parts as well. Zhu et al. had prepared Copper-based nanofluid in ethylene glycol under microwave irradiation, introducing it as the novel one step method (Zhu, Lin, & Yin, 2004)

2.8.3 Other methods:

Typically, nanofluids are stabilized by the use of surfactants or dispersants. By adding surfactants, the surface tension of the fluids containing the nanoparticles is reduced, which leads to increased immersion of the particles (Mukherjee & Paria, 2013). The surfactant used is determined by the characteristics of the nanoparticles and the basic fluid. Nonionic

detergents, for example, are frequently used to disperse metallic nanoparticles in water-based solutions.

2.9 Experimental analysis:

An experimental investigation was recently conducted by (Ali, EI-Leathy, & Al-Sofvany, The effect of nanofluid concentration on the cooling system of vechicles radiator, 2014)researched on Toyota Yaris's engine cooling mechanism by addition of Al_2O_3 in the coolant fluid. The concentration used was 1% and the heat transfer coefficient reached maximum at that point as suggested by the data obtained. The further increase in concentration would deteriorate the performance of the cooling mechanism hence making the radiator less efficient. (Nguyen, Roy, Gauthier, & Galanis, 2007) conducted an experimental research on the effects of addition of Al_2O_3 in the coolant as well. The examination of convective heat transfer efficiency along with the change in concentration of nanoparticle showed that more than 40% increase was seen in the overall heat transfer coefficient. Another study based on real life application was carried out by Pak and Cho where they studied effect of addition of $TiO_2$and Al_2O_3in a volumetric concentration os 1-3% in the overall cooling mechanism of vehicle radiator. The effect on thermophysical properties was studied. The Nusselt number was found to be increased with the increase in rate of nanoparticle concentration (Pak & Cho, 1998). Yasin et al. conducted experimental works in the internal combustion engine. Al_2O_3 particles was added to the coolant in different concentrations. The study was carried out to enhance the heat transfer performance. The enhancement was achieved upto 37.2% (at 1% concentration). Lowest overall heat transfer coefficient was found to be 2% (at 0.25% concentration) (Karagoz, 2022). Researched to investigate the convective heat transfer and pressure drop using Alumina-water nanofluid. The used test section was 1.1m long and 5 mm inner diameter tube of a double-pipe heat exchanger. The volume concentration of 0.15%, 0.25% and 0.5% were used. The maximum increase in Nusselt number was found to be 40.5% in comparison to pure water under 0.5% concentration (Sudarmadji, Soeparman, Wahyudi, & Hamidy, 2014) .

2.10 Characterization of Nanoparticle

After synthesis of nanoparticle, the characteristic feature of the obtained material must be conducted to make sure the specimen is the proper type of particle that the study is supposed to be carried out on. Therefore, before executing the practical applications of nanoparticles, it is important to properly characterize nanoparticle. As in most of cases, the size of nanoparticles is substantially smaller than the wavelength of visible radiation or visible lights(400-700nm), they cannot be observed by normal microscopes. So to even observe them, electron microscopes such as Transmission Electron Microscope (TEM) or Scanning Electron Microscope (SEM) are required. With these devices, nanoparticles can be characterized according to their shape and sizes. Along with the electron microscopic methods, there are other methods such as X-ray diffraction (XRD), X-ray photoelectron spectroscopy (XPS), X-ray absorption (XAS), Dynamic Light Scattering (DLS), Nuclear Magnetic Resonance (NMR) spectroscopy and Fourier-transform infrared (FTIR) spectroscopy, which are used according to the demand of study. (Sarker & Nahar, 2022).

Characterization of nanomaterials for any studies has a crucial role for any work being conducted on it. It is a difficult part of study as the resources available in general labs are not built for the particles that are nano-sized. But with the advancement in technology, it is possible to study the atomic structure, chemical reactivity, chemical composition etc. of almost all nanomaterials. (Rose, 2015). However, the study is mainly based on the surface properties of the nanomaterials and when it comes to the complex structures such as the toxicity studies, it becomes almost impossible to study the features without the use of two or more methods at the same time or simultaneously in the same sample. The material properties is hugely influenced when the dimensions tends to approach the low nano-range. This fact is a gateway for the study of all kinds of nanomaterials and a breakthrough for development of range of advanced products with previously thought as unrealistic qualities in a material. Meanwhile, this also brought concerns about these unique properties being a risk for human health and the environment as well. (Cornelis & Lahive, 2021). From these risks and concerns for human health, ERA (Environmental Risk Assessment) of Nanomaterials was established as a subject for research aimed majorly to study and reduce adverse effects of Nanomaterials in Complex environment systems.

UV-Vis-NIR Spectroscopy

It covers the ultraviolet-visible-near infrared spectrum. It is the study of electronic absorption where the electronic structure details is obtained through optical spectra. It operates by focusing on the electronically excited states of atoms of materials and gives the photon replica of the provided sample. The sample can be optically characterized from the measure of their spectral extinction behavior. The relative wavelength corresponding to the plasmon resonance results in enhanced near field absorption at resonance wavelength. Thus, providing local variations in permittivity of the particle, nanoparticle coupling effects, non-uniformity in nanoparticle size, aggregation phenomena as well as nanoparticle geometry (Manuel, 2022).

UV-Vis spectroscopy being a valuable tool for identification, characterization and study of nanomaterials provides a method to compare the measured spectrum with the predicted spectrum of given sample based on numerical models. There can be differences occurring during the UV-Vis spectroscopy for plasmonic and non-plasmonic nanomaterials as non-plasmonic nanoparticles have size and concentration dependent optical properties which can affect the outcome given by the machine. However, the spectrum of non-plasmonic nanoparticles is not as sensitive to dispersion as plasmonic ones (Nanoparticle Characterization Techniques, 2022).

When the light source hits the monochromator and a radiation light is sent to the specimen, the ground level atoms of the sample gets to excited state and it causes the energy level of the atom to fluctuate which is obtained in the screen in form of energy levels with the change in wavelength of the radiation sent into the monochromator. This process gives us information on the morphology of the specimen. UV test is generally done for either the qualitative or the quantitative analysis of the specimen provided according to the demand of study (UV-Vis Spectrophotometer, 2020).

Band gap

Band gap is the distance between the conduction band and the valence band of electrons of an atom. It is the energy gap or the energy range where no electronic states exist. It is normally defined for semi-conductors. When the atoms of semi-conductors get enough

energy to overcome the band gap, they become conductors. Thus, band gap shows the minimum energy required to get an electron in excited state enough to make the atom or the whole element conducting (Band Gap, 2015). So, band gap is an essential measure to study the conducting characteristic of any element

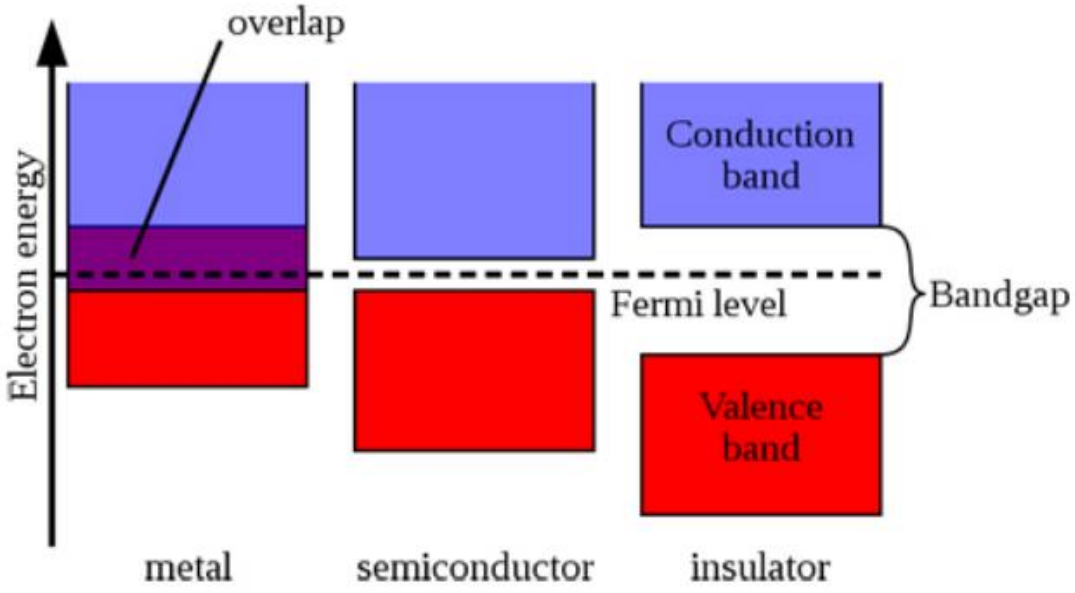

.Figure 4 Band gap diagram showing band gaps for conductors, semiconductors and insulators (Langelandsvik, 2017)

The data obtained from the UV spectroscopy gives us information regarding the absorbed energy from the energy dissipated from the monochromator along with the change in wavelength of the radiation. Then the band gap is determined by drawing a tangent line with the curve obtained. If the band gap value meets the desired range of energy gap of certain elements, then it gives the confirmation on whether the specimen is composed of the elements that is required for the experimental study.

X-Ray Diffraction

XRD is another method of characterization of nanoparticles which uses an X-ray diffractometer to study and analyze the crystalline structure of nanomaterials. The parallel beams of X-ray beam is generated from the XRD device and is directed onto the required

sample. The sample or nanoparticle should not be sensitive to the X-radiation else the properties can be altered by this process. The projected and scattered X-ray from the crystals within the sample creates an XRD pattern in powder form. This powder XRD pattern helps in the identification of atomic orientation and thus the crystal structure of nanoparticles. This provides the elemental composition of the sample crystal which helps in the further studies of nanomaterials. (Mudalige, et al., 2019).

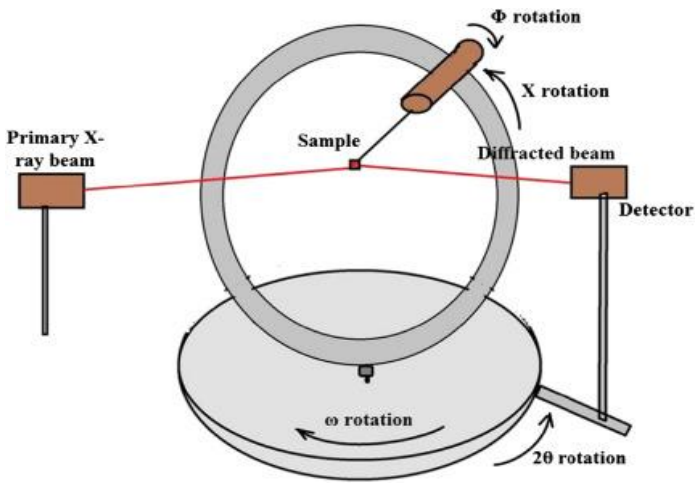

Figure 5 Representative diagram of XRD technique *(Nutan & Dhoble, 2021)*

Fourier Transform Infrared (FTIR) Spectroscopy

It is a technique used for characterization of nanoparticles majorly on the basis of surface property. It is used to obtain the infrared spectrum of emissivity, absorption capacity and photoconductivity of solid, liquid and gaseous state of materials. It opens up a gateway for the identification of characteristic functional group from the spectral band that further clears path for the conjugate relation between nanomaterial and adsorbed molecules (Lin, Lin, Wang, & Sridhar, 2014). It provides information regarding the wavelength and the intensity of adsorption. The peak intensity gives a direct indication of the nature or the behavioral characteristic shown by the material. (Kong & Yu, 2007) FTIR spectrum is recorded in different energy levels namely near-IR (400-10 cm^{-1}) , mid-IR(4000-400 cm^{-1}) and far-IR(14,000-4000 cm^{-1}). IR photons contain enough energy in them to cause

vibration of group of atoms with respect to the bond that binds them together. The photons when hit by Infrared radiation gets excited which is detected by the detector (Dutta, 2017).

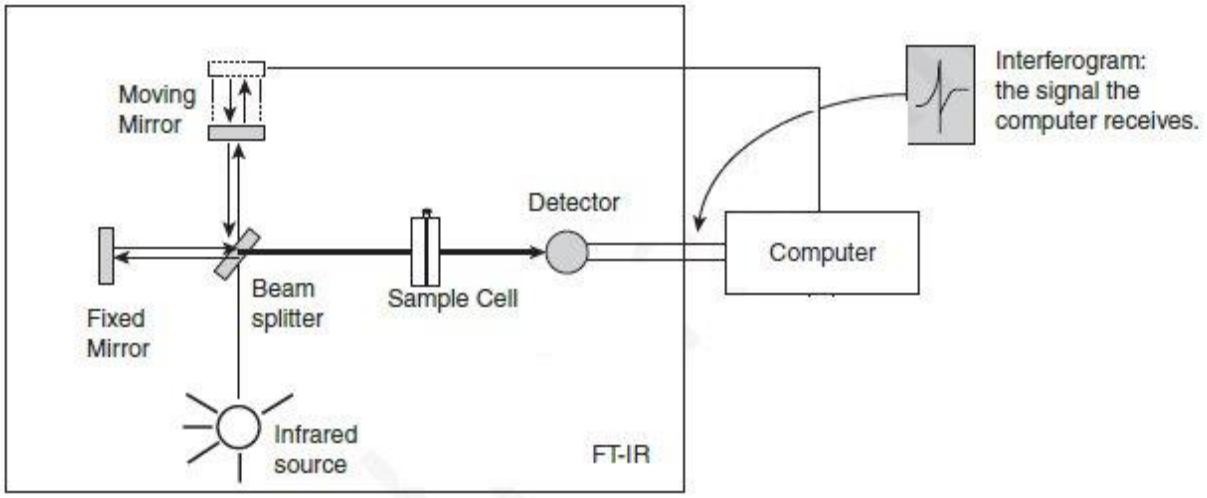

Figure 6 Schematic diagram of FTIR spectrophotometer *(Jalvandi, 2016)*

2.11 Nanofluids as coolant

Water is traditionally used as radiator coolant in automobiles. The mixture of Ethylene Glycol (EG) and water essentially form the coolant that is currently in use in most of the vehicular cooling system. However, the current demand of market has gone through the roof and the conventional form of coolant is not able to fulfill the requirement of people and the overheating engines of modern days. With the development of modern technologies, the heat transfer must be improved in automobiles which can be done by the addition of nano fluids (Jinsiwale & Achawl, 2018).

The nanofluids thermal conductivity depends upon the thermal conductivity and concentration ratio of nanoparticles and base fluid (Hwang, et al., 2007) .The heat transfer coefficient also changes with the changes made in volume, composition and environmental conditions. Thus, if not stored properly, the nanoparticle may lose its properties with time and change in other parameters. Even when the nanofluids are used by mixing with the conventional coolant, the properties might be lost during the dispersion or the mixing process which can also be a cause for unexpected minor efficiency losses.

The nanoparticles Al_2O_3 is normally chosen for the enhancement of properties in coolant as the varying volumetric concentration display a crucial increase in the average heat transfer coefficient. The change in Reynold's number, however, displays a greater influence in the positive change in the heat transfer ability of a fluid. So, using a metallic oxide nanoparticle whose property can be varied to achieve the required heat transfer coefficient suitable for the task is used in general (Vaijha, Das, & Namburu, 2010).

Experimentally the heat transfer rate increases about 40% with addition of 1% volume concentration of nanoparticles Al_2O_3 keeping Reynolds number and mass flowrate constant and overall heat transfer based on air side increased up to 36% (Kothvale & Karad, 2014). The thermal conductivity, density and viscosity increases with increase in the volume concentration. However, as the temperature increases the viscosity and density was found to be decreased (Elias, et al., 2014) . Experiment conducted shows with the 90:10 and 80:20 mixture of water-EG with 0.1% Nanofluid Al_2O_3enhances the heat transfer performance around 37% and also increases the overall heat conductance (Nambeesan, et al., 2015) . Enhancement of the thermal conductivity depends on the size of the nanoparticles, concentration and the thermal conductivity of the base fluid and also addition of small amount of Al_2O_3 increases the thermal conductivities (Xie, Wang, Xi, Liu, & Ai, 2002) .

In addition to Al_2O_3, another metallic compound SiO_2 can be used as nanoparticle additive in the coolant. Due to its lightweight and cheaper availability in market, it can be used as well. When used in real life applications, at specified conditions, it shows better outcome than Al_2O_3 as well (Mukherjee, Halder, Ranjan, Bose, & Chakrabarty, 2021). So, the field of nano particles is not just limited to any single compound but is a large field of science which keeps growing with the advancement of study and research. The more research activity is carried out, the more technologically sound and fine solution might be obtained for the required purpose.

The nanoparticles also show better results when used by mixing with Ethylene Glycol rather than mixing it with water. When mixed with EG in a calculated ratio by volume, the nanoparticles show the required property the best. The direct mixture of nanoparticles with water can even create issues regarding the stability of compound as the nanoparticles can

be unstable in normal conditions when the solution starts to disperse and flow through the cooling system. However, the unstable property of nanoparticle still prevails when used with Ethylene Glycol. There are various reasons which causes the instability of nanoparticles. They exist in a state far from equilibrium due to their high surface energy. The strong Van Der Waal's force of attraction between the surface molecules makes it difficult for the materials to stay in stabilized state. So, they can easily react with any substance near to it 7-which can cause undesired changes in the chemical or physical properties of the material (Xu, Liang, Yang, & Yu, 2018).

An experiment conducted by Eastman et. Al showed that the thermal conductivity of base fluid Ethylene Glycol with 0.3% concentration ratio of (Cu) nanoparticles, in comparison to ethylene glycol (EG) can be improved by 45%. The study conducted in Alumina based nanofluid also had similar outcome in their study (Eastman, Choi, Li, & Thompson, 2001). The addition of nanoparticles enhancing the thermal heat conductivity can be a great discovery for the cooling system mechanism of automobile industries and can be a revolutionary development in this field. Xuan and Li in 1999 published a paper describing the two step-method for nanofluid preparation and also calculated the thermal conductivity of the fluid. Effect of nanoparticles in nanofluid through their application has been studied and published in detail by them. They have used hot-wire method to determine the thermal conductivity and found that for the Copper-water nanofluid, the thermal conductivity had increased by 24% to 78% when the concentration of nanoparticle increased from 2.5% to 7.5% by volume. This showed that the heat transfer coefficient or the conductivity of the fluid increased with the increase in amount of nanoparticle added to the base fluid. They also conducted a similar study on Alumina (Al_2O_3) – water nanofluid and transformer oil-copper nanofluid, and as a result, they both showed the similar trend. Their paper also includes the relation with shape of particle with the heat transfer capacity i.e., the lower the sphericity of particles, the better heat transfer property is shown by the particle (Xuan & Li, 2000).

Experiment involving addition of Al_2O_3 nanoparticles in ethylene glycol and water by Hashemabadi et.al. conducted in radiator coolant and performance comparison with the base fluid alone showed the increase in heat transfer with addition of Al_2O_3 up to 1% by

volume. A significant increase in heat transfer capacity of the coolant of 40% was seen. This increased the Nusselt number of the fluid flow up to 40%. They concluded that the heat transfer of radiator through coolant was highly dependent on the concentration of nanoparticle and weakly dependent on the temperature difference (Hashemabadi, Peyghambarzadeh, Hoseini, & Jamnani, 2011).

The effect of addition of nanographite in heavy duty diesel engine coolant was studied by Zhang et al. They found that the heat transfer capability of coolant for cooling the engine increased by 15% when 3% by volume of nanographite was added to the existing coolant. (Zhang, et al., 2007). The effect of nanofluid based coolant in a truck engine studied by Saripella et. Al. showed that 50/50 mixture of ethylene-glycol and water used as base fluid and addition of 2 % and 4% volume of CuO particles resulted in lower power consumption of vehicle. The effect of nanofluid based coolant in the engine's temperature, pump's speed and power was studied. The addition of nanographite contributed to the reduction of pump speed up to a factor of two in comparison to the heat transfer without the addition of nanographite which was due to the less heat transfer required which eventually was because of better performance by the coolant (Saripella, Yu, Routbort, France, & Rizwan-Uddin, 2007).

Vasu et. al have also used aqueous form of alumina as coolant in automobile flat tube plain fin compact heat exchanger. The radiator that has been designed for Ethylene Glycol has been utilized for the Aluminum based nanofluid(Al_2O_3) as coolant which gave the conclusion that the heat transfer rate will decrease with the rise in air inlet temperature when used the given coolant (Vasu, Ramakrishna, & S. Kumar, 2008). Another study conducted in 2010 in automobile radiator which used Al_2O_3 and CuO as Nanoparticles for the base fluid mixture of Ethylene Glycol and water. This gave the outcome that the addition of nanoparticle in the base fluid resulted in less power required by the pump to pump the coolant into the passages hence saving power and energy losses within the engine. This is due to the increase in the heat transfer coefficient of the coolant. Thus to obtain the similar amount of heat transfer in the base fluid, less pumping force is required (Vajjha, Das, & Ray, 2015).

For the improvement of thermal conductivity of the coolant, Elias et al. conducted an experimental study by adding Al_2O_3 as nanoparticle in the mixture of Water and ethylene glycol in 0-1% by volume concentration. The study showed that the maximum improvement in the thermal conductivity of nanofluid was found to be 8.3% increase at 0.1% volume concentration while the temperature was maintained at 50^o C (Elias et. al., 2014). Ali et al. conducted experiment by using MgO as nanoparticle and mixing it with softened water to produce nanofluid as a mixture of MgO/Water with concentration of nanofluid in the range of 0.05-0.12% by volume. It was observed that the maximum enhancement in the heat transfer with the MgO nanofluid was 1.31% at 0.12% volume concentration and at maintained coolant flow rate of 8-16 l/min (Ali, Azhar, Saleem, Saeed, & Saieed, 2015).

Minsta et al studied the effect of change in size of nanoparticles, varying concentration of nanoparticles in the base fluid and the changing temperature on the thermal conductivity. The nanofluid used for experimental study were Al_2O_3/water and CuO/water. They showed that the increase in concentration of nanoparticles can efficiently improve the thermal properties of the fluid. Also, the nanoparticle of smaller sizes resulted in higher thermal conductivity at the same concentration ratio (Minsta, Roy, Nguyen, & Doucet, 2009). Another experiment-based study conducted in a Chevrolet Suburban diesel engine radiator used CuO/water nanofluid at concentration of 2% volume. The size of nanoparticle was limited to 20nm and the numerical study indicated that the overall heat transfer coefficient and pumping power of the engine were approximately 10% and 23.8% more than that of the base fluid(water) at 6000 Reynolds number whilst the speed of automobile was kept constant at 70km/hr (Bozorgan, Krishnakumar, & Bozorgan, 2012).

In a study conducted by Pantzali et al., the effects of addition of nanoparticles in base fluid or coolant of a radiator was observed experimentally. Nanofluid made essentially from CuO at 0.04% concentration by volume was passed through miniature PHE (electronic colling-liquid system). The flow of coolant was determined as mildly turbulent. The addition of nanoparticle in the base fluid had increased the heat transfer rate by about 20% in comparison to the normal coolant used in the system (Pantzali, Kanaris, Antoniadis, Mouza, & Paras, 2009). Another study incorporating Al_2O_3 as nanoparticle conducted by

Wen and Ding was done by maintaining the samples at 0.6%, 1% and 1.6% concentration by volume. The nanofluid was made by mixing Ethylene Glycol/water solution with calculated amount of Al_2O_3 to create the required nanofluid samples. The coolant was then passed through heated horizontal tube of 4.5mm internal diameter in laminar flow type. The outcome showed overall increase of 47% in the heat transfer rate when the concentration of nanoparticle was 1.6% (Wen & Ding, 2004).

CHAPTER 3 METHODOLOGY

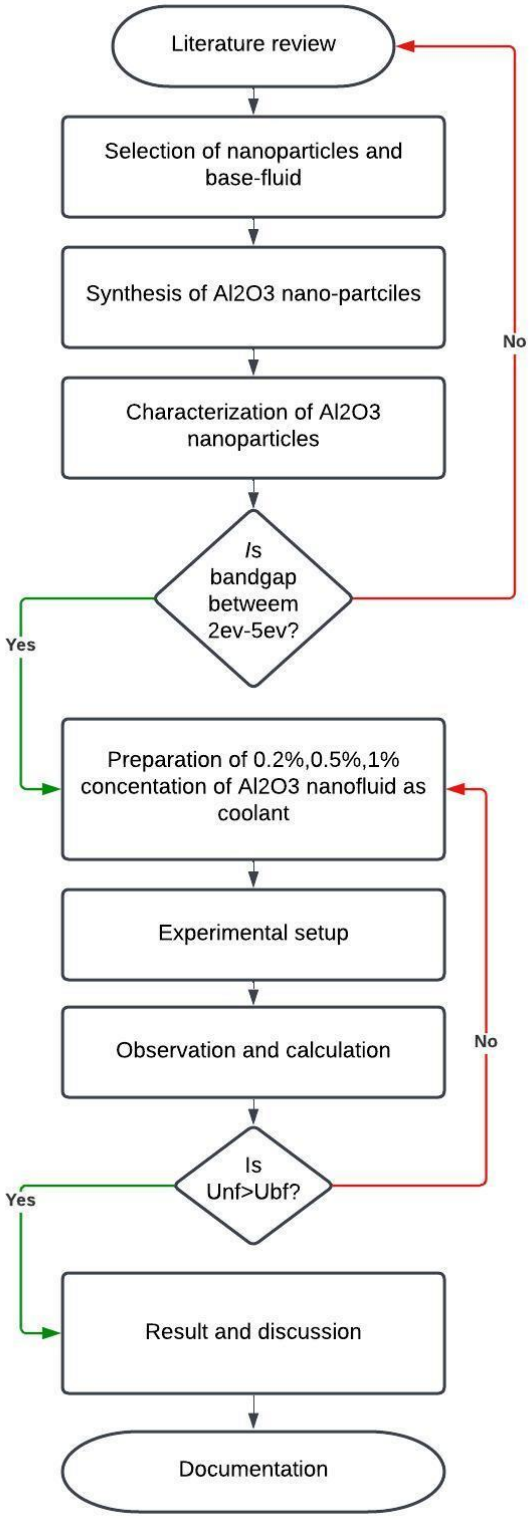

Figure 7 Flow chat of methodology

3.1 Selection of nanoparticle

From the literature review it was found that the best coolant to use for the experiment would be Ethylene Glycol because it showed the best performance while using for the nanoparticle based experiment. It is the best base fluid for mixing with nanoparticle because of the antifreeze property. Due to this property, the boiling point of the fluid increases and the freezing point decreases. This prevents the coolant from boiling at high temperatures and from freezing at extreme cold environment. In this context, we had used "MAK Super Cool" coolant as base fluid. It was recommended by the manufacturer (TATA) for TATA Tiago XZ^{+}. In addition, the coolant had additives from the manufacturers to make it anticorrosive and add antifreeze property to enhance the performance of cooling system efficiently.

For the nanoparticle, as it was seen from different studies and experiments conducted that the use of Al_2O_3 had been relatively more efficient than other nanoparticles. Alumina being more durable, more stable and it's surface property being favorable for our experiment, it was the nanoparticle used for the study. Synthesis of Alumina was also synthesizable from the available resources as Sole gel method was possible in the laboratory. Higher stability of Al_2O_3 also played a crucial role in the choice taken by us for the experiment as the nanoparticle was to be characterized and further processed into nanofluid for which being stable was important.

3.2 Synthesis of Nanoparticle

Solgel method was used for the preparation of $A\ l_2O_3$ nanoparticle. The Sol-gel method is a chemical technique that converts liquid precursors, often metal alkoxides or metal chlorides, into solid materials. The process involves hydrolysis, condensation, and aging, resulting in the formation of a three-dimensional network of solid particles that has trapped the liquid in its pores, known as a gel. The name Sol-gel originates from the two states of matter involved in the process, sol and gel. The precursor molecules are first broken down into smaller fragments through hydrolysis, followed by condensation to form larger molecular units. Finally, aging allows the gel to solidify into its final state. This method has diverse applications in materials science, electronics, optics, and biotechnology and can produce materials with controlled porosity and surface properties.

The following is a general procedure for the preparation of nanoparticles using the sol-gel method:

- Selection of Precursor: Suitable precursor material should be selected according to the desired properties of nanoparticle. It can be in the form of metal salts, metal oxides, or organic compounds.
- Preparation of Sol: Dissolve the precursor material in a suitable solvent (e.g., water, ethanol, or a combination of both) to form a sol. The concentration of the precursor material in the sol will depend on the desired particle size and the specific properties of the precursor.
- Gelation: Add a gelation agent (e.g., acid or base) to the sol to induce gelation. The gelation agent will cause the precursor to undergo hydrolysis and condensation reactions, resulting in the formation of a three-dimensional network of interconnected nanoparticles
- Aging: Allow the gel to age for a period of time to promote particle growth and maturation.
- Drying: Remove the solvent from the gel by drying at a low temperature. This can be achieved by evaporation or freeze-drying.
- Calcination: It is necessary to heat the dried nanoparticles to a high temperature in order to remove any residual organic matter and improve the crystallinity of the particles.
- Characterization: Finally, the nanoparticles can be characterized using various techniques such as X-ray diffraction (XRD) and UV-V spectrophotometer test to determine their size, shape, and other properties.

  In the experiment, above mention procedure was followed for making Al_2O_3 nanoparticle. The material and instruments which are used for the preparation of nanoparticle using the procedure is listed below.

  1. Anhydrous Aluminum Chloride as percussor
  2. Ethanol (As Solvent)
  3. Distilled water (For hydrolysis)
  4. 28% of Ammonia (Gelation Agent)
  5. Magnetic Stirrer

6. Oven
7. Beaker

The Flowchart of the procedure is shown below

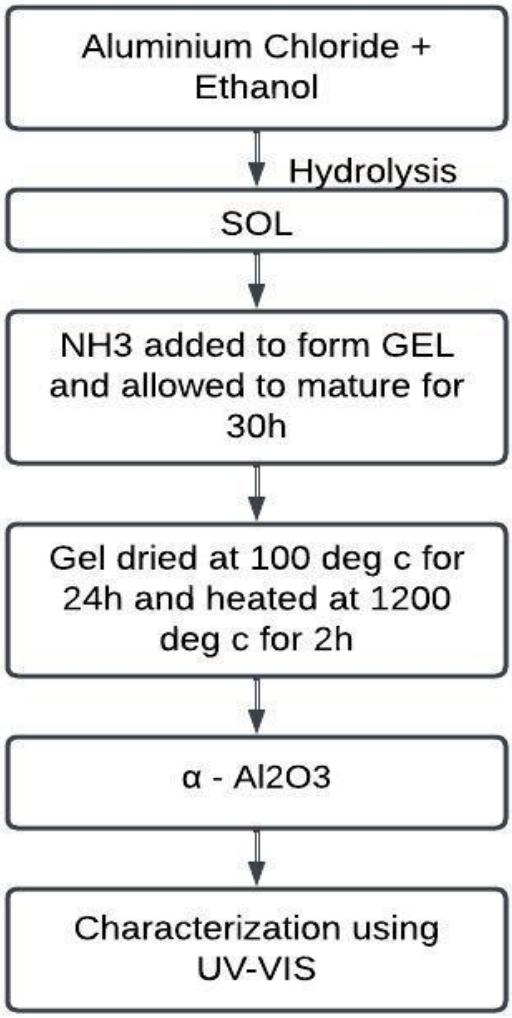

Figure 8 Flow chart of nanoparticles synthesis

The suitable precursor that has been used for making Al_2O_3 nanoparticle in this experiment is Alumunium chloride ($AlCl_3$). At first, 13.34 gram of $AlCl_3$ was weighed and taken in beaker and then 300ml of ethanol was added to it as the dissolving agent to prepare the $AlCl_3$ethanolic solution.

Figure 9 300ml Ethanol and 13.34gm Aluminum Chloride

In order to dissolve the Aluminum chloride completely in Ethanol, magnetic stirrer is used. The solution was stirred for 30 minutes using the magnetic stirrer.

A magnetic stirrer, sometimes known as a flea, is a laboratory tool used to generate a rotating magnetic field that causes a magnetic stir bar to spin quickly, stirring the liquid in a container. An electric motor-generated spinning magnetic field surrounds a small bar magnet inside the device. The stir bar, which is positioned inside the liquid, receives the magnetic field through the container's bottom. The liquid is fully and uniformly stirred as a result of the stir bar's rapid spinning caused by the revolving magnetic field may be managed.

Figure 10 Magnetic Stirring of Ethanolic Solution of Aluminum Chloride

After the magnetic stirring was done, 50ml of distilled water is added to the solution for hydrolysis and the formation of Sol takes place after the hydrolysis. After the formation of Sol, 50 ml of 28% N$H_3$was added to the Sol as the Gelation agent. The gelation agent will cause the precursor to undergo hydrolysis and condensation reactions, resulting in the formation of a three-dimensional network of interconnected nanoparticles. After the formation of gel, it was allowed to age for 30hr at room temperature to promote particle growth and maturation. Later the gel was dried at 100 degrees Celsius for 24hr in an oven to remove the solvent from gel.

Figure 11 Formation of Gel after drying

After the formation of gel, it was heated at 1200 degree Celsius for 2hr in an oven in order to remove any residual organic matter and improve the crystallinity of the particles. Finally, after calcination $A\,l_2O_3$ nanoparticle was formed which is shown in figure below.

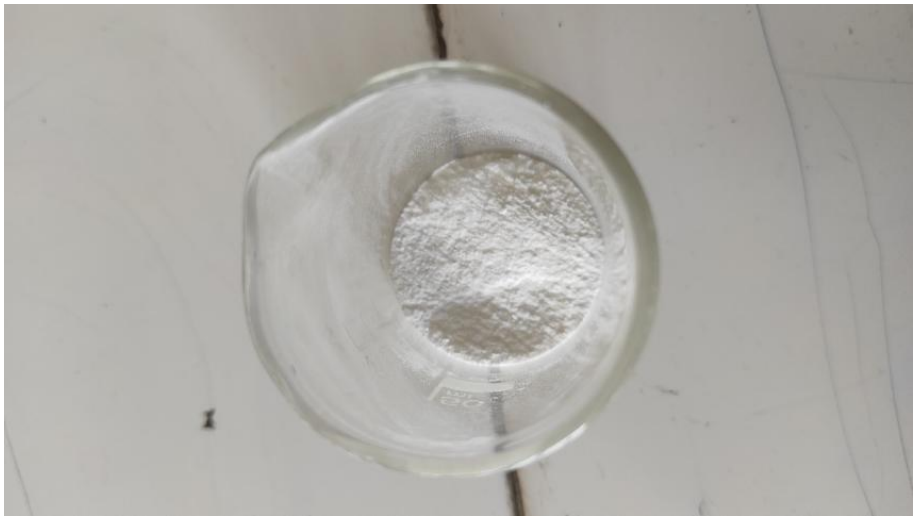

Figure 12 Nanoparticles

The chemical reaction that takes place during the preparations of $A\,l_2O_3$ nanoparticles are written below:

$$AlCl_3 + C_2H_5OH \rightarrow Al(OC_2H_5)_3 + HCl$$

$$Al(OC_2H_5)_3 + H_2O \rightarrow C_2H_5OH + Al(OH)_3$$

$$2Al(OH)_3 \rightarrow \text{AlO (OH)} \rightarrow \gamma - Al_2O_3 + \alpha - Al_2O_3 \rightarrow \alpha Al_2O_3$$

3.3 Characterization of Nanoparticle

3.3.1 UV-Visible Nanoparticle analysis

Nanoparticles are frequently examined using UV-V is spectroscopy, particularly to determine their absorption and scattering characteristics in the ultraviolet and visible portions of the electromagnetic spectrum. Depending on their makeup, shape, and size, nanoparticles can display distinctive optical characteristics when they are exposed to light. For instance, metal nanoparticles can exhibit plasmon resonance, a process in which the nanoparticle's electrons fluctuate collectively and strongly absorb light at a particular wavelength. The concentration, size, and form of the nanoparticles may be determined by measuring the absorbance or transmittance of light through a sample containing nanoparticles using UV-V is spectroscopy. Also, by evaluating the direction and strength of scattered light, UV-V is spectroscopy may be used to examine the scattering characteristics of nanoparticles.

The main purpose of the UV test of nanoparticle is to confirm the formation of $A\,l_2O_3$ nanoparticle, to find out if there are any impurities present in the sample and also with the help of the band gap, we can predict the stability of the mixture while making nanoparticles. The band gap of a material is the energy difference between its valence band and conduction band. The interaction between the nanoparticles and the host material can be influenced by the band gap when nanoparticles are combined with other substances like polymers or solvents.

The energy required to drive an electron from the valence band to the conduction band is large if the band gap of the nanoparticles is likewise high. The nanoparticles' ability to interact with the host material and produce a stable combination may be hampered as a result. In other cases, the large band gap might also make the nanoparticles less reactive.

On the other hand, if the nanoparticles' band gap is small, less energy is needed to drive an electron from the valence band to the conduction band. As a result, a stable mixture may be formed more easily and the interaction between the nanoparticles and the host material may be enhanced. Consequently, it is crucial to take into account how the band gap of the nanoparticles affects their mixing behavior when creating nanoparticle-based composites.

The amount of light absorbed by a sample over a range of wavelengths in the ultraviolet and visible portions of the electromagnetic spectrum is measured using a UV-Vis spectrophotometer. The following illustration demonstrates how a UV-Vis spectrophotometer determines a material's band gap:

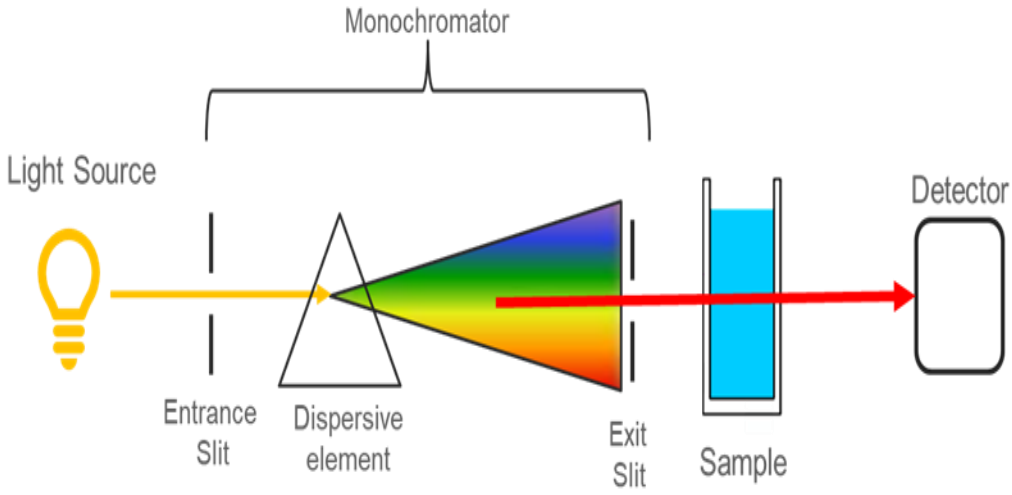

Figure 13 Schematic Diagram for working principle of the UV- Vis Spectrophotometer *(Instrumentation of a UV-Visible Spectrophotometer, 2023)*

In the Figure 13, we can see the schematic diagram of how the UV- V spectrophotometers work. It consists of a light source, monochromator, sample holder, detector and a data processing unit. The working principle is explained in detail below.

- **Light source:** A tungsten-halogen or deuterium lamp, which generates light in the ultraviolet and visible ranges of the electromagnetic spectrum, is commonly used as a source of light in UV-V spectrophotometers. Electromagnetic radiation from the light source is directed to the sample via the ultraviolet-visible spectrophotometer system. The system may be configured to either reflect light off

of the sample or transmit light through it. The light is then captured and measured after it has interacted with the sample. In this experiment tungsten- halogen lamp is used.

- **Monochromator:** Choosing a particular wavelength of light from the source is done with a monochromator. It is made out of a rotating diffraction grating or prism that controls the wavelength of light that passes through it. The entry slit of the monochromator receives the source's light first. A dispersing component, such an optical grating, is then used by the monochromator to divide the light into its individual wavelengths.
- **Sample Holder:** The substance being studied is contained in the sample holder, which may be a solution or a thin film on a substrate. The sample is illuminated by the monochromator, and the amount of light that is reflected or absorbed by the sample is measured. Here the sample taken in our case is in the form of thin film on a substrate as it gives more accurate reading than the solution. A little quantity of Al_2O_3 nanoparticle was placed above $BaSO_4$ and it was uniformly dispersed across $BaSO_4$ with the aid of a glass rod. Initially, the $BaSO_4$ was placed in a sample holder and evenly distributed in the holder and it was pressed with the help of a glass rod. The sample is compressed since the reading of the wavelength data will change if the sample of Al_2O_3 nanoparticles fall within the UV-V spectrophotometer. In UV-V spectrophotometry, BaSO4 is frequently employed as a reference material because it is a stable, insoluble white compound that uniformly reflects all light wavelengths. It is a perfect benchmark for the absorption of other compounds since it does not absorb any UV-Vis light. In a UV-Vis spectrophotometer, light is split into two routes during the measurement of absorbance, with one channel traveling through the sample and the other path travelling through the reference material. The spectrophotometer can calculate the sample's absorbance at a given wavelength by comparing the quantity of light absorbed by the sample to the amount absorbed by the reference material. Since BaSO4 is less sensitive to changes in temperature, humidity, and pressure than other frequently used reference materials like water or air, it is favored over them.

Also, because it is non-toxic and inert around the majority of chemicals, it is secure and dependable.

Figure 14 Sample placed on BaSO4 Powder

- **Detector:** The detector of a UV-Vis spectrophotometer is in charge of calculating the amount of light that has gone through the sample.
- **Data Processing unit:** The data processing unit of a UV-Vis spectrophotometer is in charge of logging the amount of light detected as a function of wavelength, which creates an absorption spectrum for the sample. The band gap energy of the material may then be inferred indirectly from this spectrum analysis by making a Tauc plot.

In this way the UV-v spectrophotometer measures the band gap of the Sample. The overall flowchart of the process is shown below.

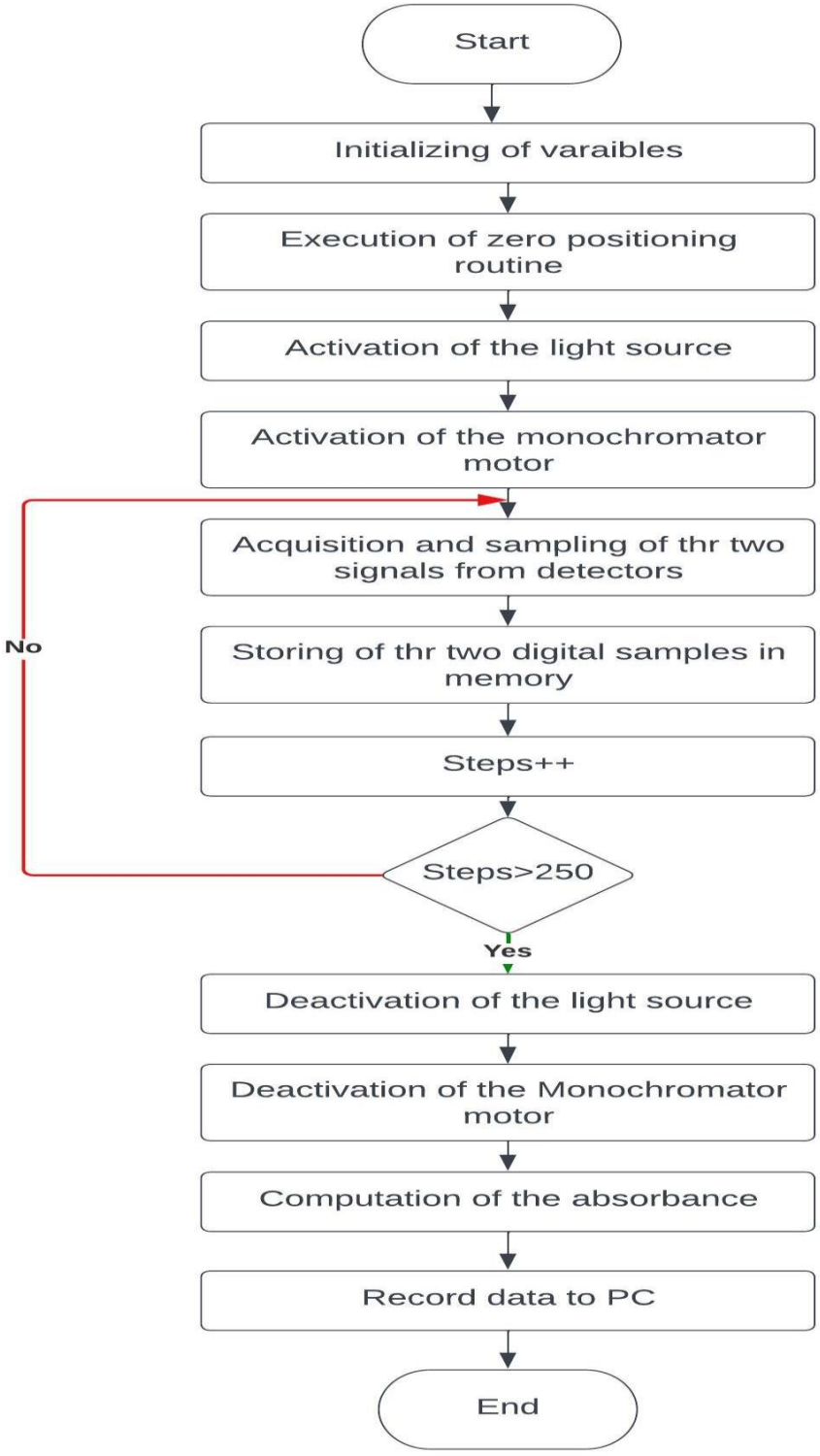

Figure 15 Flowchart of the UV test *(Design and workinh of UC-Vis Spectrophotometer, 2020)*

So, the sample holder was mounted in the UV-VIS-NIR spectrophotometer after the placement of nanoparticle on BaSO4 and the diffuse reflectance spectra o the sample we prepared were recorded in the pc in the excel form. The measurement condition and the graph of diffuse reflectance spectrum with wavelength is shown below

Measurement Wavelength range	200nm to 700nm
Sampling pitch	1.0nm
Scan speed	Medium
Slit width	20nm

Table 1 Analytical Condition

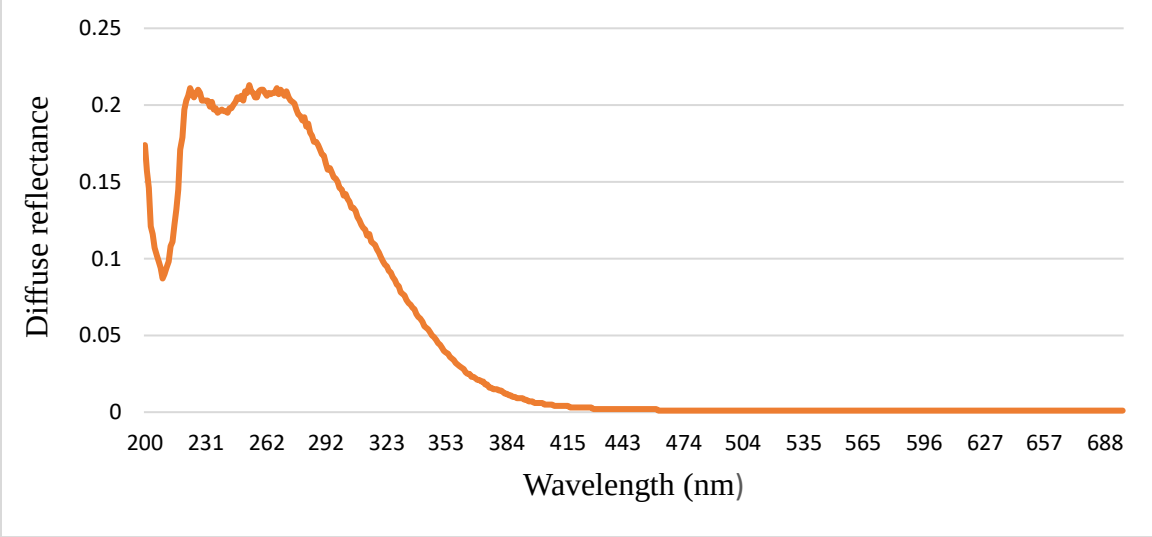

Figure 16 Diffuse reflectance spectra

After the value of diffuse reflectance spectra is measured, the band gap of Al_2O_3 is calculated using the tauc plot. Tauc plot is the most popular method for measuring the band gap from the diffuse reflectance spectrum. The procedure for the measurement of band gap using tauc plot is explained below.

1. The following formulation from Tauc, Davis, and Mott is employed.

$$(h\nu\alpha)^{1/n} = A(h\nu - Eg) \ldots\ldots\ldots\ldots\ldots\ldots\ldots\ldots\ldots\ldots (1)$$

Where:

h: Planck's constant, v: frequency of vibration, α: absorption coefficient, Eg: band gap, A: Proportional constant

The value of the exponent n denotes the nature of the sample transition.

For direct allowed transition……. n=1/2

For direct forbidden transition……... n=3/2

For direct forbidden transition……n=2

For direct allowed transition……. n=3

As this experiment employs the direct permitted sample transition, n=1/2 is used for these samples.

2. The kubelka-Munk function is created from the collected diffuse reflectance spectrum. As a result, the quantity $F(R\infty)$., which is proportional to the absorption coefficient, is translated from the vertical axis $F(R\infty)$ is used to replace in the Tauc equation. Thus, the relational expression changes in the real experiment.

$$(h\nu F(R\infty))^2 = A(h\nu - Eg) \ldots\ldots\ldots\ldots\ldots\ldots\ldots (2)$$

3. The $(h\nu F(R\infty))^2$ was plotted against the hv using the Kubelka-Munk function. A line is created to represent the curve that depicts the value of $(h\nu - h\nu F(R\infty))^2$ on the horizontal axis hv and vertical axis $(h\nu F(R\infty))^2$.
   When hv is expressed in terms of electron volts (eV), its connection to wavelength (λ)nm is changed to hv = 1239.7/λ.
4. A line is drawn tangent to the point of inflection on the curve of step (3) and the hv value at the point of intersection of the tangent line and the horizontal axis is the band gap Eg value.

The recorded data shown in appendix 1 is used and wavelength is converted in terms of electron volts using step 3 formula mentioned above. Then the graph is plotted that depicts the value of $(h\nu - h\nu F(R\infty))^2$ on the horizontal axis hv and vertical axis

$(hvF(R\infty))^2$and the tangent is drawn in the curve at the point of inflection by following step 3 and step 4 and the graph is shown below.

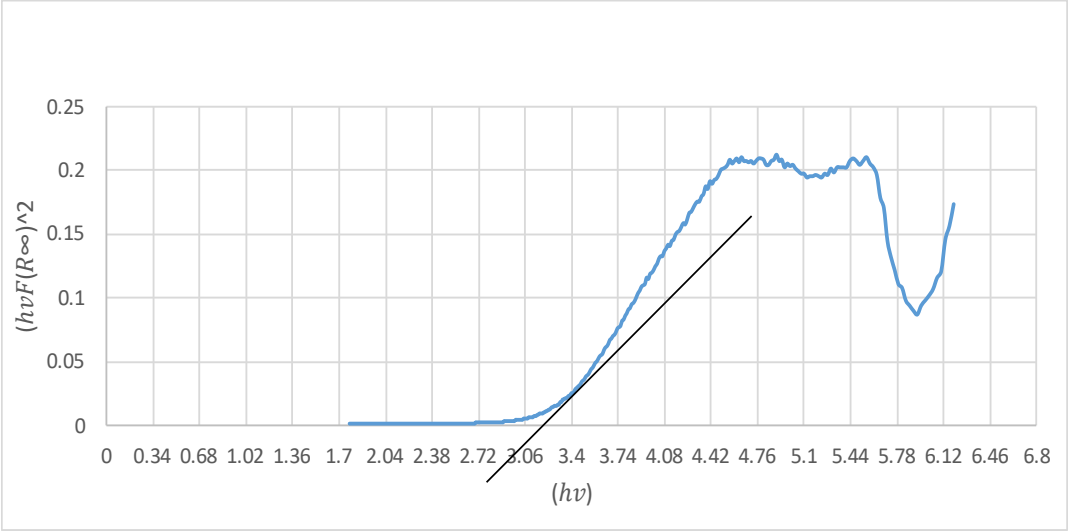

Figure 17 $(hv - hvF(R\infty))^2$ curve of $A\ l_2O_3$ nanoparticle

From the figure 17, we can clearly see that the tangent line cuts the x-axis in between 3.06 and 3.4ev and we know that the point of cut tangent line at x axis give the value of band gap, hence the value of band gap of $A\ l_2O_3$ nanoparticle obtained is 3.23ev (383.8nm). In this way the band gap of the $A\ l_2O_3$ nanoparticle is found out. The graphical pattern shown by the test confirms the formation of the $A\ l_2O_3$ nanoparticle and Fig 16 also shows that the sample doesn't contain any other compounds or impurities since there is no such irregular peak shown in graph after 300nm wavelength. Following graph were obtained from the data provide in Appendix A.

3.4 Synthesis of nanofluid:

A nanofluid was created in two steps using 0.2%, 0.5%, and 1% concentrations of Al 2 O 3 nanoparticles in a basic fluid of 33.33% coolant and 66.67% purified water. The two-step technique for creating nanofluids involves individually synthesizing nanoparticles and the base fluid, then merging the two components to make the nanofluid. Three samples of nanofluid were created, each having 4 liters of base fluid and a different concentration of nanoparticles Al_2O_3.

First batch preparation: For a 0.2% concentration of nanoparticles, 0.4 grams of Al 2 O 3 were weighed to guarantee appropriate dispersion for experimental analysis. The 0.4 gram was split into two portions, and the basic fluid was made into two liters using the proper ratio. First, 0.2 grams of Al 2 O 3 nanoparticles were distributed in purified water before the coolant was introduced. The dispersion procedure took about four hours, and the 0.2% Al 2 O 3 nanofluid was kept in the same beaker after dispersion. The most feasible method for dispersion was to use a magnetic stirrer and devote identical time to each of the 0.5% concentration side by side dispersion operations. The base fluid, consisting of 33.33% ethylene glycol and 66.67% distilled water, was divided according to the division of the nanoparticles i.e., 2666 lit distilled water and 1334 lit ethylene glycol.

Second batch preparation: After the completion of first batch second batch was prepared accordingly to achieve an appropriate dispersion of nanoparticles. 1 gram of Al_2O_3 were weighed out to create a 0.5% concentration. This amount was then divided into two parts and mixed with a base fluid consisting of two liters, prepared with the appropriate ratio. The base fluid was a combination of 33.33% ethylene glycol and 66.67% distilled water, which was divided proportionally based on the nanoparticle division, which means 2666 liters of distilled water and 1334 liters of ethylene glycol were used. Initially, 0.5 grams of Al_2O_3 nanoparticles were dispersed using distilled water, followed by the addition of the coolant. The dispersion process lasted approximately four hours, and the resulting nanofluid containing 0.5% Al_2O_3 was kept in the same beaker.

Third batch preparation: In this batch, a 1% concentration of nanoparticles was used to prepare the nanofluid, and the same procedure as the first batch was followed for the third batch. To achieve the desired concentration, 2 grams of Al_2O_3 was weighed out and divided into two parts along with the base fluid, which helped ease the dispersion process. The dispersion process was carried out for about four hours with the help of a magnetic stirrer. To ensure uniform dispersion, equal time was allocated to each of the side-by-side dispersion processes for the 1% concentration, and after dispersion, the nanofluid was stored in the same container. The basic fluid used for the nanofluid was a mixture of 33.33% ethylene glycol and 66.67% distilled water, which was proportionally split based on the

nanoparticle partition. This resulted in 2666 liters of distilled water and 1334 liters of ethylene glycol.

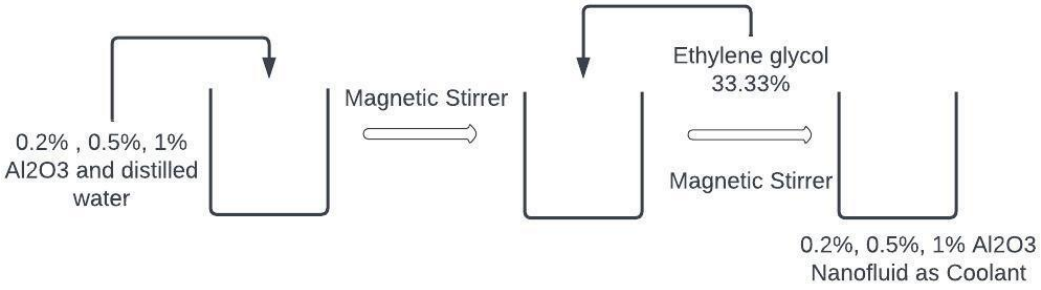

Figure 18 synthesis of nanofluid of different concentration

The dispersion of nanoparticles plays a crucial role in experimental analysis as it is essential for maintaining the stability of the nanofluid. Achieving proper dispersion can be a time-consuming process. Therefore, to ensure nanoparticles are uniformly distributed throughout the base fluid in every batch, they are divided based on their concentration. Similarly, the base fluid is also divided accordingly. For instance, 2666 liters of distilled water is divided equally into two parts, 1333 liters each, while 1334 liters of coolant (ethylene glycol) is divided into two parts of 667 liters each. Before the experiment, all the nanofluids were again dispersed for 30 -30 mins, to make sure there is not any disposal. It is essential to use a base fluid with a high thermal conductivity and low viscosity to achieve maximum efficiency in heat transfer applications.

Figure 19 Synthesis of nanofluid using magnetic stirrer

3.5 Experimental Setup:

For the experimental analysis the vehicle TIAGO XZ+-2016 model with 1199 cc engine is used for the study of effect of nanoparticles. The petrol engine present in the vehicle consists of 4 cylinder and is a DOHC engine. The maximum power generated by the vehicle is 84 BHP(@6000 rpm) and the maximum torque generated is 114 Nm(@3500 rpm) (Tata Motors Product, n.d.).

Figure 20 TATA Tiago XZ^{+}

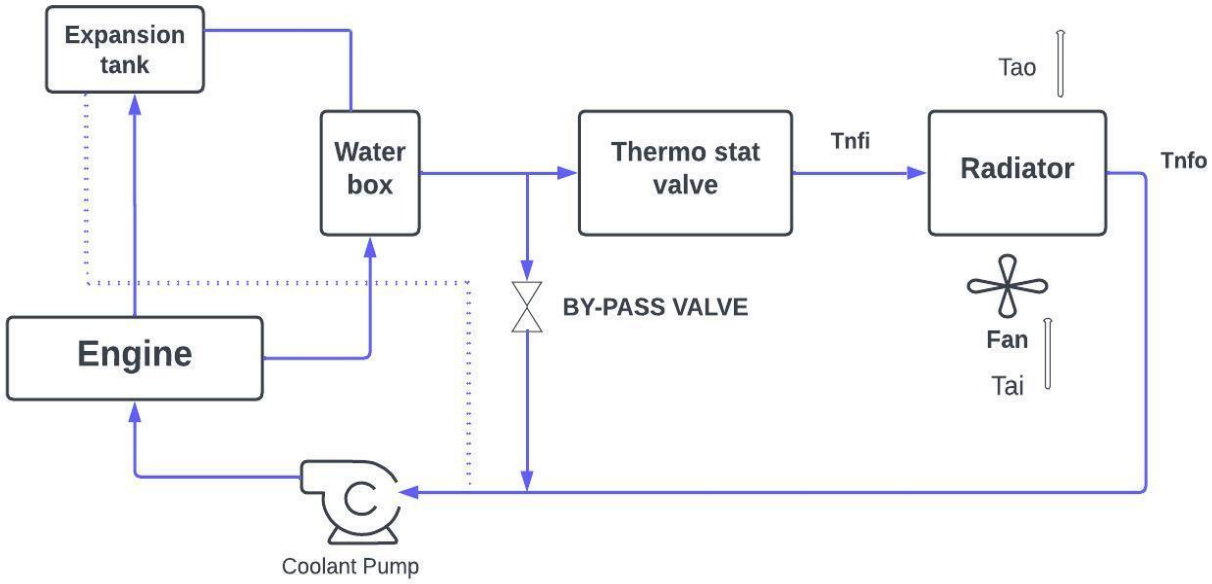

Figure 21 Schematic Diagram of Experimental Setup

This is a schematic representation of the experimental setup used to determine how nanofluids affect a vehicle's radiator. Internal combustion engine, vehicle radiator, pump, flow lines, thermostat valve, and expansion tank are among the experimental systems used in research. Sensors are installed to detect the temperature reading and mass flow rate, and the results of the experiment displayed immediately on the computer screen as shown in Figure 21. At the radiator's input and output, the temperatures of the cooling liquid and air are monitored. The amount of heat the engine rejects to the cooling fluid varies with engine speed. Therefore, the cooling fluid inlet temperature changes as the speed of the engine changes.

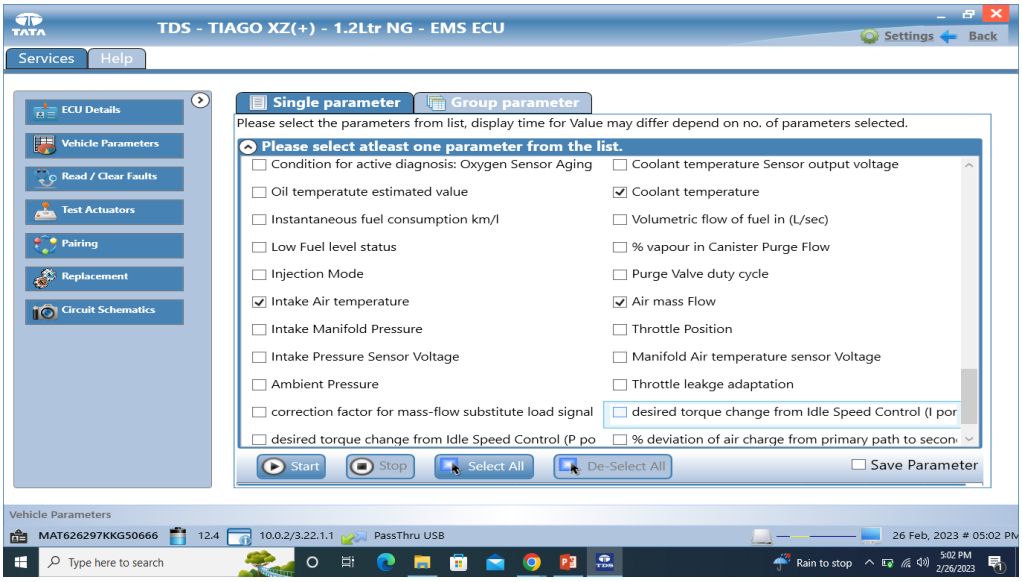

Figure 22 Data recording at PC

The study involved using two test liquids: Ethylene Glycol and water. Initially, the base fluid was tested. Then, an engine test was conducted where the engine speed was gradually increased to 2500 rpm, causing the coolant to heat up. Once heated, the coolant was allowed to cool while recording relevant data on a computer. After that, the coolant was drained from the radiator and replaced with a nanofluid prepared for use as the coolant. The air Reynolds number and coolant mass flow rate were kept constant at predetermined values throughout the investigation. However, the Al_2O_3 nanoparticle concentration varied from 0% to 1%. Three different volumes of nanofluid, 0.2%, 0.5%, and 1%, were used as samples, and the experiment was repeated for each sample to determine how the addition of nanoparticles affected the base fluid's heat transfer performance.. The assumptions that have to be made during the testing procedure is mentioned below

- Velocity and temperature at the entrance of the radiator core on both air and coolant sides are uniform.
- There are no phase changes (condensation or boiling) in all fluid streams
- Fluid flow rate is uniformly distributed through the core in each pass on each fluid side

Both the air Reynolds number and coolant mass flow rate will be held constant throughout the investigation at predetermined values. Al_2O_3 nanoparticle concentration, however, went from 0% to 1%. The radiator's efficiency, overall heat transfer coefficient, and total heat transfer were calculated.

3.5.1 Calculation of thermal properties of base fluid

The thermal properties i.e., density, specific heat capacity, thermal conductivity and viscosity, were calculated of base fluid in order to compute the experimental data. The thermal properties of water at 85^o are (Evans, 2015):

- Density: 0.96862g/cm^3
- Specific heat capacity:4.120 KJ/kg.k
- Viscosity: 0.00033 Pa.S
- Thermal conductivity: 0.673W/m.k

Similarly thermal properties of ethylene glycol at 85^o are (The Engineerig ToolBox, 2001), (Ethylene Glycol product Guide, 2018):

- Density:1.1499 g/cm^3
- Specific heat capacity:2.43KJ/Kg.K
- Viscosity:0.002566 Pa.S
- Thermal conductivity:0.1386 W/m.K

Density ($\boldsymbol{\rho_c}$):

Density of base fluid= (volume percentage of Water* density of water +volume percentage EG*density of EG)

$$\rho_b = 0.3333 \times 1.1499 + 0.6667 \times 0.96862$$

$$= 1.025 \text{g}/cm^3$$

Therefore, the estimate density of the mixture at 33.33:66.67 (by volume) is 1.017 g/cm^3 at 85^o.

Specific heat capacity ($\boldsymbol{Cp_c}$):

$$Cp_c = 0.3333 \times 2.43 + 0.667 \times 4.120$$

= 3.55723 KJ/Kg.K

Thermal conductivity (k_c):

$$Thermal\ conductivity\ of\ mixture\ at\ 85^o$$
$$= (Thermal\ conductivity\ of\ ethylene\ glycol \times Volume\ fraction\ of\ ethylene\ glycol) + (Thermal\ conductivity\ of\ water\ glycol \times Volume\ fraction\ of\ water)$$

$$Thermal\ conductivity\ of\ mixture\ at\ 85^oC$$
$$= 0.1386 \times 0.33 + 0.673 \times 0.667$$
$$= 0.4945\ W/m.k$$

Viscosity(μ_c):

The dynamic viscosity of the mixture at 85°C using the Wilke's mixing rule as:

$$(Viscosity\ of\ mixture)/(Viscosity\ of\ water) = \Phi EG \times (Viscosity\ of\ Ethylene\ glycol)/\Phi EG \times (Viscosity\ of\ Ethylene\ glycol) + \Phi W \times (Viscosity\ of\ water) + \Phi W \times (Viscosity\ of\ Water)/(\Phi EG \times (Viscosity\ of\ ethylene\ Glycol) + \Phi W \times (Viscosity\ of\ water) \times sqrt(M\_EG/(M\_W)$$

where, $M_{EG}\ and\ M_W$ are the molecular weights of Ethylene glycol and water, $\Phi EG\ and\ \Phi W$ are the volume fraction of ethylene glycol and volume fraction of water.

$$(Viscosity\ of\ mixture)/(Viscosity\ of\ water) = 0.3333 \times (0.002566)/(0.3333 \times (0.002566) + 0.6667 \times (0.00033) + 0.6667 \times (0.00033)/(0.3333 \times (0.002566) + 0.6667 \times (0.00033) \times sqrt(62.07/18.02)$$

$$(Viscosity\ of\ mixture)/(Viscosity\ of\ water) = 1.2581$$

$$Viscosity\ of\ mixture = 1.2581 \times 0.00033$$

$$= 0.0004151\ Pa.s$$

Therefore, the viscosity of the mixture with 33.33% volume of ethylene glycol and 66.67% volume of water is approximately 0.0004151 Pa·s at 85°C.

3.5.2 Calculation of thermal properties of Nanofluid fluid:

Thermal properties of nanoparticles are:

S. no.	Properties	Al203
1	Density (ρ_p)(Kg/m^3)	3950
2	Specific heat (c_p)(J/kg K)	873.336
3	Thermal Conductivity (k_p)	31.922
4	Viscosity (N/sm^2)	-

Table 2 Nanoparticles properties (Kothvale & Karad, 2014)

The thermal properties, density, specific heat and viscosity of nanofluid were calculated from the given formulas (Ali, A.M, & Al-Sofyany, 2014) whereas thermal conductivity calculated from Maxwell-Eucken equation.

Sample-1 (0.2% concentration of nanofluid)

- Density $(\rho_{nf}) = \emptyset\rho_p + (1-\varphi)\rho_c$

$$= 0.002 \times 3950 + (1 - 0.002)1025$$

$$= 1030.85\ \text{kg/m}^3$$

- Specific capacity $(C_{nf}) = \frac{\emptyset\rho_p c_p + (1-\emptyset)\rho_c cp_c}{\rho}$

$$= \frac{0.002 \times 3950 \times 873.336 + (1 - 0.002) \times 1025 \times 3557.23}{1030.85}$$

$= 3536.66.2$ J/kg.k

- Viscosity $(\mu_{nf}) = \mu_c \exp \frac{4.91\emptyset}{0.2092-\emptyset}$

$$= 0.00042 \exp \frac{4.91 \times 0.02}{0.2092 - 0.002}$$

$$= 0.00042 \text{ Pa.s}$$

- Thermal conductivity $(k_{nf}) = k_c(1 + 2.5\emptyset + 1.5\emptyset\ (1 - \emptyset)(\frac{k_p}{k_c} - 1)$

$$= 0.4945(1 + 2.5 \times 0.002 + 1.5 \times 0.002(1 - 0.002)\left(\frac{31.922}{0.4945} - 1\right)$$

$= 0.59107$ W/m. K

Sample-2 (0.5% concentration of Al2O3 nanofluid)

- Density $(\rho_{nf}) = \emptyset\rho_p + (1 - \varphi)\rho_c$

$$= 0.05 \times 3950 + (1 - 0.005)1025$$

$=1039.63$ kg/m^3

- Specific capacity $(C_{nf}) = \frac{\emptyset\rho_p Cp + (1-\emptyset)\rho_c cp_c}{\rho}$

$$= \frac{0.005 \times 3950 \times 873.336 + (1 - 0.005) \times 1025 \times 3557.23}{1039.63}$$

$= 3506.24$J/kg.k

- Viscosity $(\mu_{nf}) = \mu_c exp \frac{4.91\emptyset}{0.2092-\emptyset}$

$$= 0.00042 \exp \frac{4.91 \times 0.05}{0.2092 - 0.005}$$

$$= 0.00047\ Pa.s$$

- Thermal conductivity $((k_{nf}) = k_c(1 + 2.5\emptyset + 1.5\emptyset\ (1 - \emptyset)(\frac{k_p}{k_c} - 1)$

$$= 0.4945(1 + 2.5 \times 0.005 + 1.5 \times 0.005(1 - 0.005)(\frac{31.922}{0.4945} - 1)$$

$$= 0.73521$$

Sample-3 (1% concentration of Al2O3 nanofluid)

- Density $(\rho_{nf}) = \emptyset\rho_p + (1 - \varphi)\rho_C$

$$= 0.01 \times 3950 + (1 - 0.01)1025$$

$$=1054.25\text{kg/m}^3$$

- Specific capacity $(C_{nf}) = \frac{\emptyset\rho_p Cp+(1-\emptyset)\rho_c cp_c}{\rho}$

$$= \frac{0.01\times3950\times873.336+(1-0.01)\times1025\times3557.23}{1054.25}$$

$$= 3456.671\ \text{J/kg.k}$$

- Viscosity $(\mu_{nf}) = \mu_c \exp\frac{4.91\emptyset}{0.2092-\emptyset}$

$$= 0.000415\ \exp\frac{4.91 \times 0.01}{0.2092 - 0.01}$$

$$= 0.000531\ \text{Pa.s}$$

- Thermal conductivity $(k_{nf}) = k_c(1 + 2.5\emptyset + 1.5\emptyset\ (1 - \emptyset)(\frac{k_p}{k_c} - 1)$

$$= 0.4945(1 + 2.5 \times 0.01 + 1.5 \times 0.01(1 - 0.01)\left(\frac{31.922}{0.4945} - 1\right)$$

$$= 0.97356$$

3.5.3 Experimental data analysis:

The car radiator used in this experimental study is tubular, cross-flow radiator as shown in the figure. The dimensional study of the radiator of the engine was taken and used for the design purpose and calculation propose It consists of 47 vertical tubes made of aluminum, the height of the radiator is h=0.450 m, the length of radiator is L=0.609m and the thickness

of fin is t=0.025m. The number of air passages is 99 and tube thickness is 0.005mm and are 10mm in diameter. For the performance analysis of the car radiator is analyzed using LMTD (Long Mean Temperature Difference) method which is (Ali, A.M, & Al-Sofyany, 2014) defined as follows:

$$Q_{ave} = UAF\Delta T_{lm} \ldots\ldots\ldots\ldots\ldots\ldots\ldots\ldots\ldots 3$$

where U is the overall heat transfer coefficient, A is the surface Area, and F is the correction factor applied to the value of ΔT_{lm}.

To find Q_{ave} , coolant side heat transfer rate and heat gained by air are find out . The coolant side heat transfer rate is given by :

$$Q_c = m_c Cp_c(Tc_i - Tc_o) \ldots\ldots\ldots\ldots\ldots\ldots 4$$

where $m_c, Cp_c, Tc_i, and\ Tc_o$ are the coolant flow rate , specific heat of the coolant, coolant inlet and coolant outlet.

The heat gained by the air is given by:

$$Q_a = m_a Cp_a(Ta_i - Ta_o) \ldots\ldots\ldots\ldots\ldots\ldots 5$$

where $m_a, Cp_a, Ta_i, and\ Ta_o$ are the air flow rate , specific heat of the air, air inlet and air outlet.

The mathematical average heat transfer rate (Vithayasai, Kiatsiriroat, & Nuntaphan, 2006) is:

$$Q_{ave} = 0.5(Q_c + Q_a) \ldots\ldots\ldots\ldots\ldots\ldots\ldots 6$$

It should be noted that in an ideal scenario, the amount of heat released by the coolant should be equal to the amount of heat absorbed by the air. Nevertheless, this ideal condition was never attained due to several factors such as heat leaks and errors that occurred during experiments. This difference can be put in a heat balance equation (cite) as:

$$Heat\ balance_{ave} = \frac{Q_c - Q_a}{Q_{ave}} \times\ 100 \ldots 7$$

Now, LMTD equation is given as:

$$Q_{ave} = UAF\Delta T_{lm} \ldots\ldots\ldots\ldots\ldots\ldots\ldots 8$$

ΔT_{lm} is given as:

$$\Delta T_{lm} = \frac{\Delta T_1 - \Delta T_2}{ln(\Delta T_1/\Delta T_2)} \ldots\ldots\ldots\ldots\ldots\ldots 9$$

where $\Delta T_1 = Tc_i - Ta_i$, $\Delta T_2 = Tc_o - Ta_o$, and the correction factor is (cite)given by:

$$F = \frac{ln(1 - RS)/(1 - S)}{(1 - 1/R)ln[1 + Rln(1 - S)} \ldots 10$$

where R and S defined as:

$$R = \frac{(Ta_o - Ta_i)}{(Tc_i - Tc_o)} \ldots\ldots\ldots\ldots\ldots\ldots\ldots 11$$

$$S = \frac{(Tc_o - Tc_i)}{(Ta_i - Tc_i)} \ldots\ldots\ldots\ldots\ldots\ldots\ldots 12$$

Hence the overall heat transfer coefficient is obtained

$$U = \frac{Q_{ave}}{AF\Delta T_{lm}} \ldots\ldots\ldots\ldots\ldots\ldots\ldots\ldots 13$$

It should be noted that if A represents either the total coolant inner surface area of the tubes or the total surface area for the air side, the resulting U represents the coolant side's or the air side's overall heat transfer coefficient, respectively.

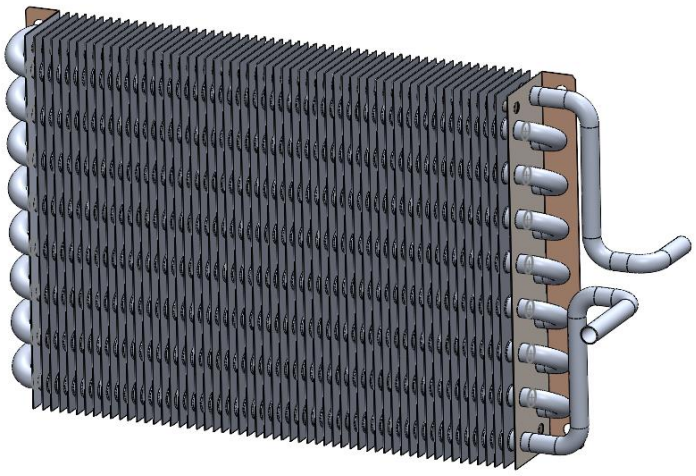

Figure 23 3-D Modeling of radiator

3.5.4 Observation and calculation:

Nanoparticle concentration	Coolant temperature		Mass flow rate (kg/s)
	Outlet	Inlet	
0 0.2 0.5 1	87.5 85.5 83.31 80	97.5 97.5 98.75 97.5	0.036
Nanoparticle concentration	Air temperature		Mass flow rate (kg/s)
	Outlet	Inlet	
0 0.2 0.5 1	41.8 43.5 45.8 47.1	36 36 36 36	0.18

Table 3 Observation table

Sample 1: 0 % concentration of Nanoparticle by volume

The coolant side heat transfer rate is given by:

$$Q_c = m_c Cp_c(Tc_i - Tc_o)$$

= 0.012*3*3557.23*(97.5 -87.5)

= 1280.60 J/s

The heat gained by the air is given by:

$$Q_a = m_a Cp_a(Ta_i - Ta_o)$$

=0.18*1005(41.8 - 36)

=1049.22 J/s

The mathematical average heat transfer rate is:

$$Q_{ave} = 0.5(Q_c + Q_a)$$

=0.5(1299.186+ 1049.22)

=1164.9114 J/s

Now,

$$Heat\ balance_{ave} = \frac{Q_c - Q_a}{Q_{ave}} \times 100$$

$$= \frac{1280.60-1049.22}{1164.9114} \times 100$$

$$= 19.81\%$$

Now,

$$\Delta T_1 = Tc_i - Ta_i$$

$$= 97.5 - 41.8$$

$$= 55.7^o\text{C}$$

$$\Delta T_2 = Tc_o - Ta_o$$

$$= 87.5 - 36$$

$$= 51.5^o\text{C}$$

LMTD equation is given as:

$$Q_{ave} = UAF\Delta T_{lm}$$

ΔT_{lm} is given as:

$$\Delta T_{lm} = \frac{\Delta T_1 - \Delta T_2}{ln(\Delta T_1/\Delta T_2)}$$

$$= \frac{55.7-51.5}{ln(55.7/51.5)}$$

$$= 47.177^o\text{C}$$

The correction factor is given by:

$$F = \frac{ln(1 - RS)/(1 - S)}{(1 - 1/R)ln[1 + Rln(1 - S)]}$$

where R and S defined as:

$$R = \frac{(Ta_o - Ta_i)}{(Tc_i - Tc_o)}$$

$$= \frac{(41.8-36)}{(97.5-87.5)}$$

$$= 0.5$$

$$S = \frac{(Tc_o - Tc_i)}{(Ta_i - Tc_i)}$$

$$= \frac{(87.5-97.5)}{(36-97.5)}$$

$$= 0.162$$

So,

$$F = \frac{\ln(1-0.081)/(1-0.162)}{(1-1/0.5)\ln[1+0.5*\ln(1-0.162)]}$$

$$= \frac{ln(1.096)}{(-1)*ln[1 + 0.5*(-0.176)]}$$

$$= \frac{0.091667}{0.09212}$$

$$= 0.99$$

Area = 0.609 * 0.025

= 0.01522 m^2

Hence the overall heat transfer coefficient is obtained

$$U = \frac{Q_{ave}}{AF\Delta T_{lm}}$$

$$= \frac{1164.914}{0.01522*0.99*(54.54+273)}$$

= 236.036 W/m^2.K

Sample 2: 0.2 % concentration of Nanoparticle by volume

The coolant side heat transfer rate is given by:

$$Q_c = m_c C_{nf}(Tc_i - Tc_o)$$

= 0.0126*3*3536.66(97.5 – 85.15)

=1651.01 J/s

The heat gained by the air is given by:

$$Q_a = m_a Cp_a(Ta_i - Ta_o)$$

=0.18*1005(43.5 - 36)

=1356.75 J/s

The mathematical average heat transfer rate is :

$$Q_{ave} = 0.5(Q_c + Q_a)$$

=0.5(1651.01+1356.75)

=1503.88 J/s

Now,

$$Heat\ balance_{ave} = \frac{Q_c - Q_a}{Q_{ave}} \times 100$$

$$= \frac{1651.01 - 1356.75}{1503.88} \times 100$$

= 19.46%

Now,

$$\Delta T_1 = Tc_i - Ta_i$$

= 97.5 – 43.5

$= 54^o C$

$$\Delta T_2 = Tc_o - Ta_o$$

= 85.15– 36

$= 49.15^o C$

LMTD equation is given as:

$$Q_{ave} = UAF\Delta T_{lm}$$

ΔT_{lm} is given as:

$$\Delta T_{lm} = \frac{\Delta T_1 - \Delta T_2}{ln(\Delta T_1/\Delta T_2)}$$

$$= \frac{54-49.15}{ln(54/49.15)}$$

$$= 52.87702\ ^{\circ}C$$

The correction factor is given by:

$$F = \frac{ln(1-RS)/(1-S)}{(1-1/R)ln[1+Rln(1-S)]}$$

where R and S defined as:

$$R = \frac{(Ta_o - Ta_i)}{(Tc_i - Tc_o)}$$

$$= \frac{(43.5-36)}{(97.5-85.15)}$$

$$= 0.607$$

$$S = \frac{(Tc_o - Tc_i)}{(Ta_i - Tc_i)}$$

$$= \frac{(85.15-97.5)}{(36-97.5)}$$

$$= 0.2$$

So,

$$F = \frac{\ln(1-0.1214)/(1-0.2)}{(1-1.647)\ln[1+0.607*\ln(1-0.2)]}$$

$$= \frac{ln(1.098)}{(-0.647)*ln[1+0.607*\ln(0.8)]}$$

$$= \frac{0.09349}{0.09705}$$

$$= 0.9638$$

$$\text{Area} = 0.609 * 0.025$$

$$= 0.01522\ m^2$$

Hence the overall heat transfer coefficient is obtained

$$U = \frac{Q_{ave}}{AF\Delta T_{lm}}$$

$$= \frac{1503.88}{0.01522*0.9638*(51.87+273)}$$

$$= 315.57 W/m^2.K$$

Sample 3: 0.5 % concentration of Nanoparticle by volume

The coolant side heat transfer rate is given by:

$$Q_c = m_c C_{nf}(Tc_i - Tc_o)$$

$$= 0.012*3*3506.24(98.75 - 83.3125)$$

$$= 1948.59 J/s$$

The heat gained by the air is given by:

$$Q_a = m_a Cp_a(Ta_i - Ta_o)$$

$$= 0.18*1005(45.8- 36)$$

$$= 1772.18 J/s$$

The mathematical average heat transfer rate is :

$$Q_{ave} = 0.5(Q_c + Q_a)$$

$$= 0.5(1948.59+ 1772.18)$$

$$= 1860.385 J/s$$

Now,

$$Heat\ balance_{ave} = \frac{Q_c - Q_a}{Q_{ave}} \times 100$$

$$= \frac{1976.98-1772.18}{1860.385} \times 100$$

$$= 9.48\%$$

Now,

$$\Delta T_1 = Tc_i - Ta_i$$

$$= 98.75 - 45.8$$

$$= 52.95\ ^{\circ}C$$

$$\Delta T_2 = Tc_o - Ta_o$$

$$= 83.3 - 36$$

$$= 47.3\ ^{\circ}C$$

LMTD equation is given as:

$$Q_{ave} = UAF\Delta T_{lm}$$

ΔT_{lm} is given as:

$$\Delta T_{lm} = \frac{\Delta T_1 - \Delta T_2}{ln(\Delta T_1/\Delta T_2)}$$

$$= \frac{52.95-47.3}{ln(52.55/47.3)}$$

$$= 50.0719^{\circ}C$$

The correction factor is given by:

$$F = \frac{ln(1-RS)/(1-S)}{(1-1/R)ln[1+Rln(1-S)}$$

where R and S defined as:

$$R = \frac{(Ta_o - Ta_i)}{(Tc_i - Tc_o)}$$

$$= \frac{(45.8-36)}{(98.75-83.3)}$$

$$= 0.6343$$

$$S = \frac{(Tc_o - Tc_i)}{(Ta_i - Tc_i)}$$

$$= \frac{(83.3-98.75)}{(36-98.75)}$$

$$= 0.24$$

So,

$$F = \frac{\ln(1-0.6343*0.24)/(1-0.24)}{(1-1/0.6343)\ln[1+0.6343*\ln(1-0.24)]}$$

$$= \frac{ln(1.115)}{(-0.57)*ln[1 + 0.6343*(-0.2744)]}$$

$$= \frac{0.105654}{-0.57*(-0.19128)}$$

$$= 0.969039$$

Area = 0.609 * 0.025

= 0.01522 m^2

Hence the overall heat transfer coefficient is obtained

$$U = \frac{Q_{ave}}{AF\Delta T_{lm}}$$

$$= \frac{1860.385}{0.01522*0.969039*(50.0719+273)}$$

= 390.42W/m^2.K

Sample 4: 1 % concentration of Nanoparticle by volume

The coolant side heat transfer rate is given by :

$$Q_c = m_c C_{nf}(Tc_i - Tc_o)$$

= 0.012*3*3456.671(97.5 - 80)

= 2177.70 J/s

The heat gained by the air is given by:

$$Q_a = m_a Cp_a(Ta_i - Ta_o)$$

= 0.18*1005(47.1 - 36)

= 2007.99 J/s

The mathematical average heat transfer rate is :

$$Q_{ave} = 0.5(Q_c + Q_a)$$

= 0.5(2177.70 + 2007.99)

= 2092.845 J/s

Now,

$$Heat\ balance_{ave} = \frac{Q_c - Q_a}{Q_{ave}} \times 100$$

$$= \frac{2177.70-2007.9}{2092.845} \times 100$$

$$= 8.1\%$$

Now,

$$\Delta T_1 = Tc_i - Ta_i$$

$$= 97.5 - 47.1$$

$$= 50.4\ ^{\circ}C$$

$$\Delta T_2 = Tc_o - Ta_o$$

$$= 80 - 36$$

$$= 44\ ^{\circ}C$$

LMTD equation is given as:

$$Q_{ave} = UAF\Delta T_{lm}$$

ΔT_{lm} is given as:

$$\Delta T_{lm} = \frac{\Delta T_1 - \Delta T_2}{ln(\Delta T_1/\Delta T_2)}$$

$$= \frac{50.4-44}{ln(50.4/44)}$$

$$= 47.177\ ^{\circ}C$$

The correction factor is given by:

$$F = \frac{ln(1 - RS)/(1 - S)}{(1 - 1/R)ln[1 + Rln(1 - S)}$$

where R and S defined as:

$$R = \frac{(Ta_o - Ta_i)}{(Tc_i - Tc_o)}$$

$$= \frac{(47.1-36)}{(97.5-80)}$$

$$= 0.63$$

$$S = \frac{(Tc_o - Tc_i)}{(Ta_i - Tc_i)}$$

$$= \frac{(80-97.5)}{(36-97.5)}$$

$$= 0.2845$$

So,

$$F = \frac{\ln(1-0.63*0.2845)/(1-0.2845)}{(1-1/0.63)\ln[1+0.63*\ln(1-0.2845)]}$$

$$= \frac{ln(1.147)}{(-0.587)*ln[1 + 0.63*(-0.3347)]}$$

$$= \frac{0.13715}{-0.587*0.23682}$$

$$= 0.99$$

Area = 0.609 * 0.025

= 0.01522 m^2

Hence the overall heat transfer coefficient is obtained

$$U = \frac{Q_{ave}}{AF\Delta T_{lm}}$$

$$= \frac{2092.845}{0.01522*0.9911*(47.177+273)}$$

$$= 433.32 W/m^2.K$$

CHAPTER 4 RESULT AND DISCUSSION

4.1 Effect of Using Nanofluid on Outlet temperature of the Coolant

In this section, analysis of thermal performance of an automobile car radiator at constant Reynolds number and constant flow rate on both air and coolant side have been carried out. The speed of the engine was increased to 2500rpm which causes the coolant to get heated. First of all, the experiment was carried out for the base fluid i.e., Ethylene Glycol and Distilled water to check the reliability of the experimental setup.

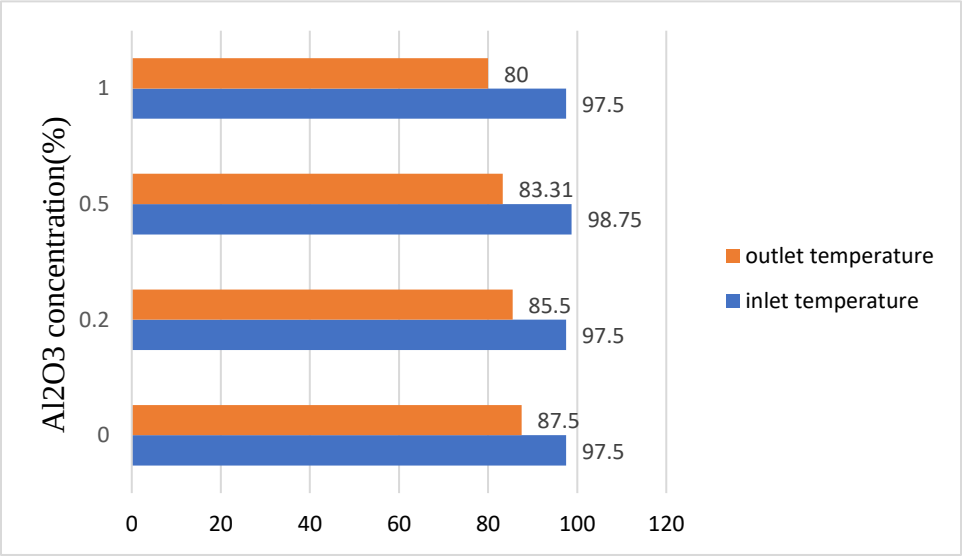

Figure 24 Temperature graph for different concentration of nanoparticle

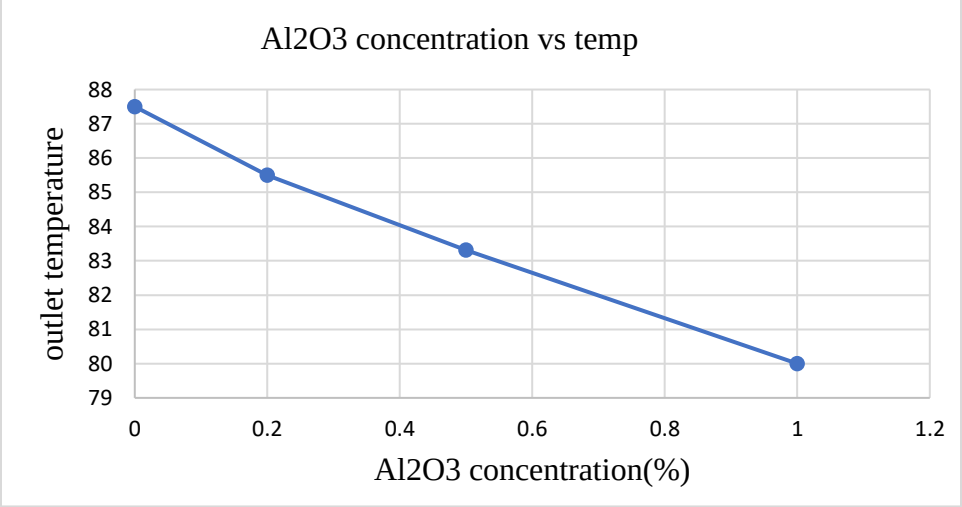

Figure 25 Effect of concentration of nanofluids on the outlet temperature

The figure 24 above indicates the temperature contour with inlet side depicted in the blue color and outlet temperature in orange color. For nanofluids with concentration of $A\,l_2O_3$ of 0% i.e., base fluid only, fluid temperature decreased from 97.5 degree Celsius to 87.5 degree Celsius. Nanofluids concentration of $A\,l_2O_3$ of 0.2% was able to reduce the temperature from 97.5degree Celsius to 85.5 degree Celsius. Furthermore, nanofluids with 0.5%percent $A\,l_2O_3$ concentration lower the temperature from 98.75 to 83.31 degree Celsius. Meanwhile, for nanofluids with 1%$A\,l_2O_3$ concentration, the temperature drop was quite high, from 97.5 degree Celsius to 80degree Celsius.

As shown in figure 25, the outlet temperature of coolant was gradually decreasing as the concentration of nanoparticle increases. The outlet temperature was quite high in case of base fluid and it was lowest for the nanofluids with 1%$A\,l_2O_3$. It shows that, the effect of nanoparticle added to the base fluid increase its thermal properties cause of which the coolant temperature decreases rapidly which indicates the improvement in the heat transfer performance of the coolant.

4.2 Effect of Using Nanofluid on Heat Transfer rate of coolant

Heat transfer involves the transfer of energy from a region of higher temperature to a region of lower temperature. The objective of heat transfer calculations is to estimate the eventual temperature of the object and the time required for it to reach that temperature. After the experiment was conducted, with the help of inlet temperature and outlet temperature heat transfer rate of coolant was calculated and the values are shown in the graph below.

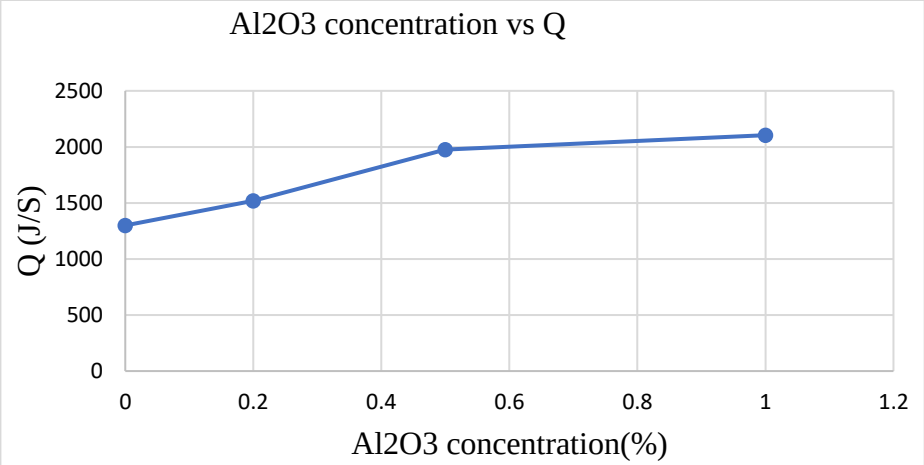

Figure 26 Effect of concentration of nanofluids on heat transfer rate of coolant

The figure 26 above indicates the heat transfer rate of coolant at different concentration of nanofluids. For nanofluids with concentration of $A\,l_2O_3$ of 0% i.e., base fluid only, the heat transfer rate was found to be 1280.60J/s which was the least value among the tested sample. Nanofluids concentration of $A\,l_2O_3$ of 0.2% was able to increase the heat transfer rate to 161.01 J/s. So, the increment of 28.92% on the heat transfer rate of the coolant was seen after the addition of 0.2% nanoparticle by volume. Furthermore, nanofluids with 0.5%percent $A\,l_2O_3$ concentration, the heat transfer rate of coolant was increased by 52.16% and found to be 1948.59 J/S. Meanwhile, for nanofluids with 1% $A\,l_2O_3$ concentration, increment by 70.85% in heat transfer rate was found and the value of heat transfer rate was 2177.70 J/S. The value of the heat transfer rate was found to be increasing at the significant rate unto 0.5%percent $A\,l_2O_3$ concentration but after that the addition of nanoparticle up to 1% there is less improvement in the heat transfer rate which suggest that addition of nanoparticle increases thermal performance up to suitable range only so the addition of nanoparticle up to only 1% by volume concentration was suggested from the above graph.

4.3 Effect of Using Nanofluid on Heat Balance Average

In an ideal case, the heat released by the coolant should be equal to heat absorbed by the air. However, this will never be possible in an experimental setup due to several factors as heat leakages and experimental errors.

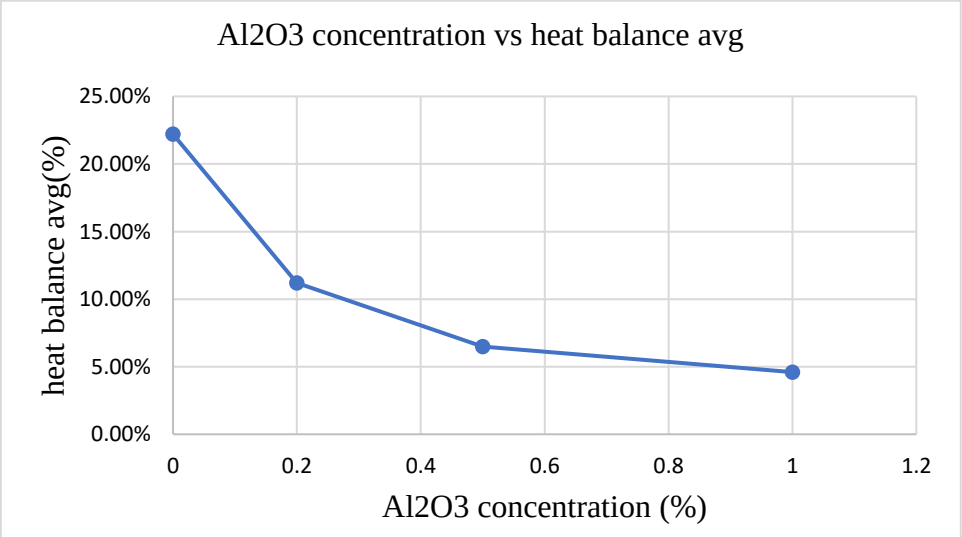

Figure 27 Effect of concentration of nanofluids on heat balance average

The figure 27 above indicates that the heat balance average error is maximum for the base fluid i.e., for nanofluids with concentration of $A\,l_2O_3$ of 0% which was about 19.81 %. Then after the addition of nanoparticle, the error in the heat balance average decreases from 19.81 to 19.46% for nanofluids with 0.2%percent $A\,l_2O_3$ concentration. For nanofluids with 0.5%$A\,l_2O_3$ concentration, heat balance averages decrease up to 9.48% and for nanofluids with 1% $A\,l_2O_3$ concentration the error was found to be 8.1 % only, which was the least error observed among the 4 sample in which experiment was carried. The graph shows that as the concentration of nanoparticle increases in volume the heat transfer from coolant to air is better cause nanoparticles have a much larger surface area to volume ratio than larger particles, which allows for increased interaction with heat transfer surfaces.

4.4 Effect of Using Nanofluid on Overall Heat Transfer Coefficient

The thermal properties of coolants were improved by the addition of nanoparticles due to various reasons. One reason is that nanoparticles have a larger surface area to volume ratio than larger particles, which can increase their interaction with heat transfer surfaces. This results in better heat transfer and ultimately improve the coolant's cooling performance. Additionally, nanoparticles possess unique thermal properties that differ from bulk materials, such as high specific surface area, thermal conductivity, and heat capacity. Moreover, nanoparticles affect the physical and chemical properties of the coolant, such as viscosity and boiling point, which can improve its stability and heat transfer efficiency and ultimately increment in the overall heat transfer can be seen as indicated by figure below.

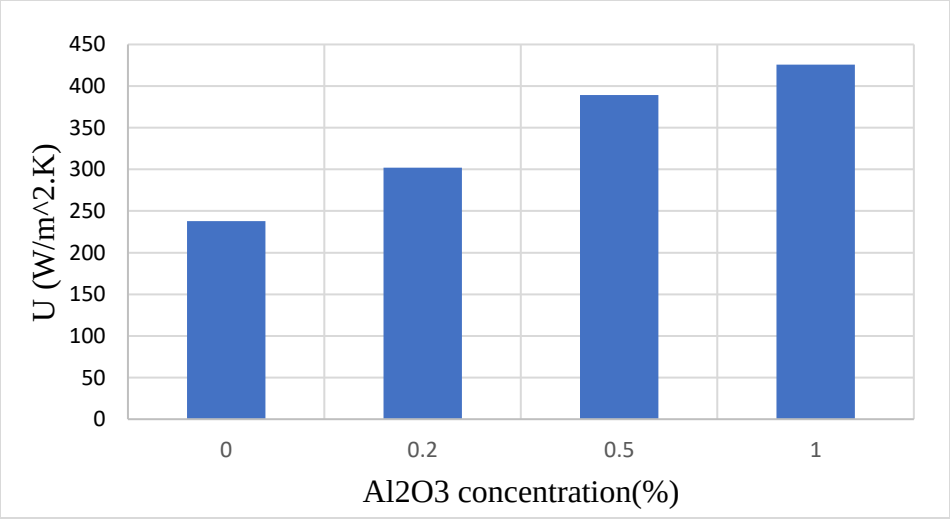

Figure 28 Effect of Using Nanofluid on Overall Heat Transfer Coefficient

The figure 28 indicates that, there is the increment in overall heat transfer coefficient after the addition of nanoparticle in the base fluid. For nanofluids with concentration of $A\,l_2O_3$ of 0% i.e., base fluid only, the overall heat transfer coefficient was found to be 236.036 W/m^2.K and after addition of 0.2 percent of $A\,l_2O_3$ nanoparticle in base fluid, the overall heat transfer coefficient was increased by 33.63% and was found to be 315.57W/m^2.k. Furthermore, For nanofluids with 0.5% $A\,l_2O_3$ concentration increment by 65.4% was seen in overall heat transfer coefficient and the value is found to be 390.42W/m^2.K . For the nanofluid with 1 percent of $A\,l_2O_3$ concentration, the value of U was found to maximum among the 4 sample and the increment of 83.5% was seen and the value was found to be 433.32 W/m^2.K. The overall heat transfer coefficient was increased by 66.23% at constant Reynold number and mass flowrate (Venkatesan, 2015) which verified the satisfactory result of the experiment result.

4.5 Effect of Using nanofluid on thermal conductivity applying Maxwell Eucken Equation

The effect on thermal conductivity by using nanofluid was found out by applying Maxwell Eucken Equation since experimental analysis couldn't be conduct due to lack of available resources. From the analytical approach, thermal conductivity was found to be increasing with increase in concentration of $A\,l_2O_3$ nanoparticle as shown in figure

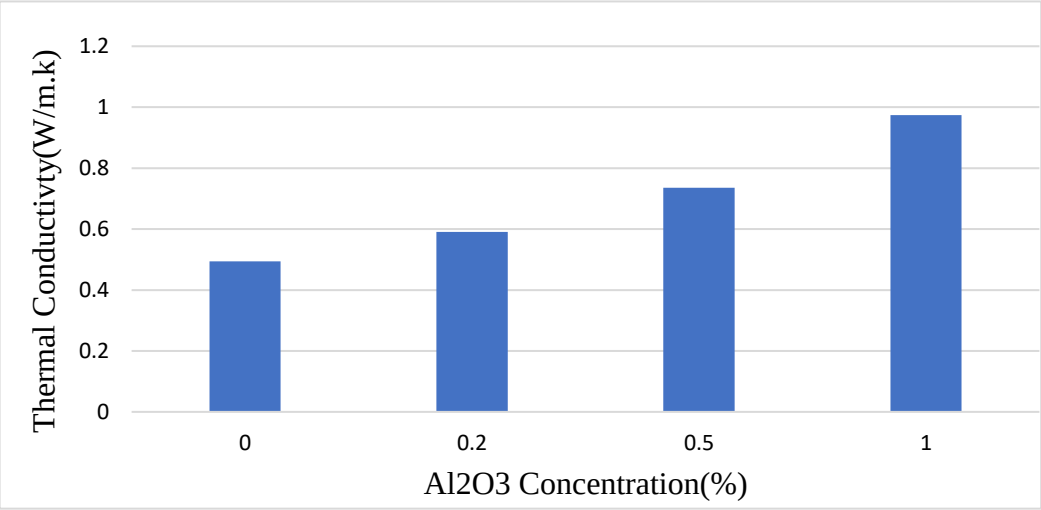

Figure 29 Effect of using nanofluid on thermal conductivity

As indicated by figure 29, the value of thermal conductivity for nanofluids with concentration of $A\,l_2O_3$ of 0% was found to be 0.4945 W/m.K and after the addition of 0.2% $A\,l_2O_3$ nanoparticle , an increment in 19.52% in thermal conductivity was seen. Furthermore, conductivity for nanofluids with concentration of $A\,l_2O_3$ of 0.5%, it was increased by 48.6% and the value was found to be 0.73521 W/m.K. The thermal conductivity was found to be maximum at 1% concentration of $A\,l_2O_3$ nanoparticle with the value of 0.97356W/m. k and the increment of 96.8% was seen. The increment in the thermal conductivity was because of special characteristic of Nanoparticle. Nanoparticles can improve the transfer of heat through the vibration of atoms in a material, known as phonon transport. This mechanism is especially effective in materials with high thermal conductivity, like metals. When nanoparticles are added to a fluid, they can act as scattering centers for phonons, which increases their mean free path and, in turn, enhances thermal conductivity. When nanoparticles are introduced into a fluid, they move randomly due to collisions with the surrounding molecules, a phenomenon known as Brownian motion. This motion can promote better mixing between the particles and the fluid, which can improve heat transfer and thus increase thermal conductivity. Adding nanoparticles in a polymer-based fluid like ethylene glycol results in interactions between the nanoparticles and the polymer chains in the fluid. These interactions create a more rigid structure that can conduct heat more efficiently.

4.6 Effect of addition of nanoparticle on Viscosity

The impact of nanoparticles on viscosity can vary depending on different factors, such as the size, shape, concentration, and surface properties of the particles, as well as the characteristics of the fluid in which they are dispersed. In general, the presence of nanoparticles can increase viscosity due to their resistance to flow, but the effect may also depend on the size and surface chemistry of the particles. This topic is currently an active area of research in the field of nanotechnology. Here, the calculation of viscosity was done by the analytical approach due to lack of resources in on experimental setup. The data calculated is shown below.

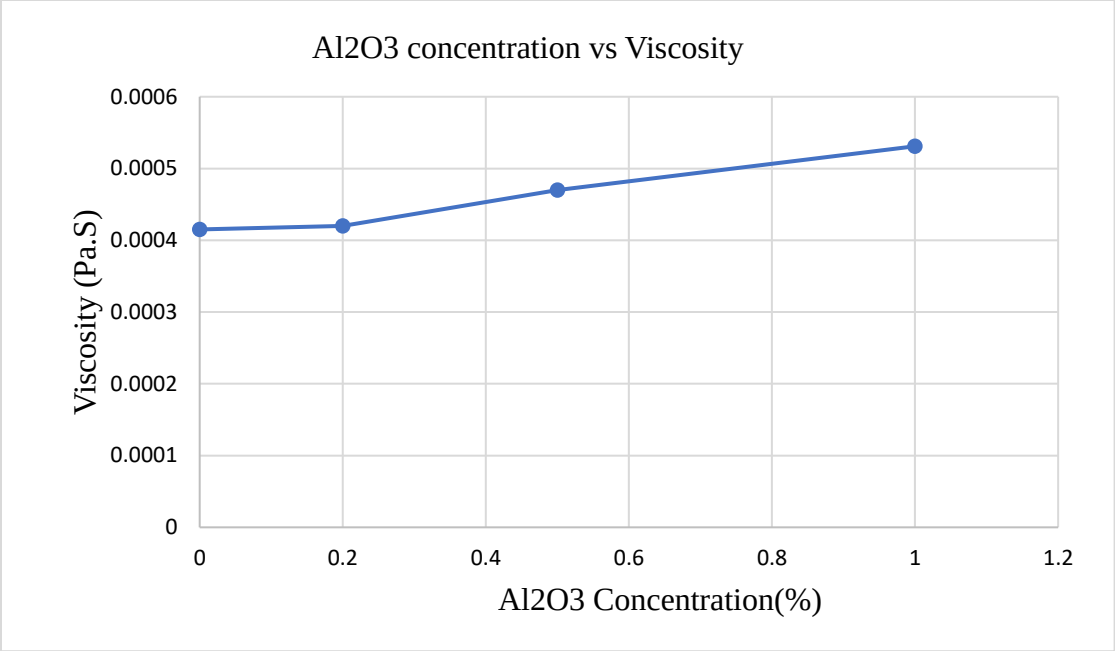

Figure 30 Effect of addition of nanoparticle on Viscosity

The figure 30 indicates that the viscosity of the coolant was found to be increasing after the addition of the Al_2O_3 nanoparticle. The viscosity was found to be minimum for the base fluid with the value of 0.000415 Pa. S and maximum for nanofluids of 1% Al_2O_3 concentration with value of 0.000531 Pa.S. It indicates that the size of the nanoparticle was high cause if the nanoparticle size was low it reduce viscosity due to their ability to form structured layers within the fluid that reduce the mobility of the fluid molecules.

CHAPTER 5 CONCLUSION AND LIMITATION

5.1 CONCLUSION

The effects of nano particles were studied from the experimental analysis of the vehicle radiator of the TATA Tiago XZ^{+}

- The nanoparticles Al_2O_3 was synthesize using two step approach method and the characterized with the UV-Vis spectroscopy where bandgap was found to be 3.23 ev.
- The outlet temperature was of each concentration was found to be decreasing with increase in concentration of theAl_2O_3 nanoparticle.
- The heat transfer rate of coolant was found to be maximum for the 1% Al_2O_3 concentration with increment of 70.85 % than the base fluid.
- The overall heat transfer coefficient of the radiator was increased after the addition of the nanoparticle and was found to be maximum for the 1% Al_2O_3 concentration with increment of 83.5% than the base fluid.

5.2 LIMITATION

- The vehicle was kept at idle condition i.e., velocity of vehicle was zero, which might have affected the nature of the data and deviated from the real-life application-based data.
- The vehicle was at unloaded condition which is also not the case during the real application of on road vehicle.
- The engine speed could not be maintained constantly at same magnitude because it is practically impossible to keep engine at same speed for longer duration.
- There is a possibility of deposits of nanoparticle being formed inside the radiator or the coolant passage inside the engine compartment due to stability issues in the nanoparticle.

REFERENCES

Ahmed, M. A., & Abdel-Messih, M. F. (2011). Structural and nano-composite features of TiO2–Al2O3 powders prepared by sol–gel method. *Journal of Alloys and Compounds*, 2154-2159.

Ali, A. R., & Salam, B. (2020). A review on nanofluid: preparation, stability, thermophysical properties, heat transfer characteristics and application. *SN Applied Sciences*.

Ali, H. M., Azhar, M., Saleem, M., Saeed, Q. S., & Saieed, A. (2015). Heat transfer enhancement of car radiator using aqua based magnesium oxide nanofluids. *Thermal Science vol. 19*, 2039-2048.

Ali, M., A.M, E.-L., & Al-Sofyany, Z. (2014). The Effect of Nanofluid Concentration on the Cooling System of Vehicles Radiator. *Advances in Mechanical Engineering*.

Ali, M., EI-Leathy, A. M., & Al-Sofvany, Z. (2014). The effect of nanofluid concentration on the cooling system of vechicles radiator. *Advannce Mechanical Engineering*.

Alwan, R. M., Kadhim, Q. A., Sahan, K. M., Ali, R. A., Mahdi, R. J., Kassim, N. A., & Jassim, A. N. (2015). Synthesis of zinc oxide nanoparticles via sol–gel route and their characterization. *Nanoscience and Nanotechnology*.

Band Gap. (2015). Retrieved from pv education: pveducation.org

Bhanvase, B., & Barai, D. (2021). Stability of nanofluids. In *Nanofluids for Heat and Mass Transfer* (pp. 69-97). Academic Press.

Bokov, D., Turki Jalil, A., Chupradit, S., Suksatan, W., Javed Ansari, M., Shewael, I. H., & Kianfar, E. (2021). Nanomaterial by sol-gel method: synthesis and application. *Advances in Materials Science and Engineering*, 1-21.

Bozorgan, N., Krishnakumar, K., & Bozorgan, N. (2012). Numerical study on application of CuO-water nanofluid in automotive diesel engine radiator. *Modern Mechanical Engineering, Vol. 2, No. 4*, 130-136.

Cabaleiro, D., Colla, D., Barison, S., Lugo, L., Fedele, L., & Bobbo, S. (2017). Heat trasnfer capability of (ethylene glycol + water)-based nanofluids containing graphene nanoplatelets: design and thermophysical profile. *Nanoscale Research Letters*.

Chaudhari, K., Walke, P., Wankhede, U., & Shelke, R. (2015). An experimental investigation of a nanofluid(Al2O3 + H20) based parabolic trough solar collectors. *British Journal of Applied Sciences and Technology*, 551-557.

Che Sidik, N. A., Mohd Yazid, M. N., & Mamamt, R. (2015). A review on the application of nanofluids in vehicle engine cooling system. *International Communications in Heat and Mass Transfer*, 85-90.

Cornelis, G., & Lahive, E. (2021). Occurence, behaviour and effects of inorganic nanoparticles in the environment. In *Comprehensive Analytical Chemistry, vol. 93* (pp. 1-34). Elsevier.

Design and workinh of UC-Vis Spectrophotometer. (2020). Retrieved from smacgigworld.

Dinesh, R., k.k., Dinesh., Haribabu, M., & Pratheesh, R. (2018). Analysing the causes of overheating of heavy duty truck engines and het flux of Radiator using Pareto Priciples Ansys Software. *International journal of pure and Applied Mathematics*, 4955-4963.

Dutta, A. (2017). Fourier Transform Infrared Spectroscopy. In *Spectroscopic methods for nanomaterials characterization* (pp. 73-93). Elsevier.

Eastman, J., Choi, S., Li, S., & Thompson, L. (2001). Anomalously increased effective thermal conductivites of ethylene glycol-based nanofluids containing copper nanoparticles. *Applied Physics Letters*, 718-720.

Elias et. al., M. M. (2014). Experimental investigation on the thermo-physical properties of AL2O3 nanoparticles suspended in car radiator coolant. *International Communications in Heat Mass Transfer vol. 54*, 48-53.

Elias, M., mahbubul, I., Saidur, R., Sohel, M., Shahrul, I., khaleduzzaman, S., & Sadeghipour, S. (2014). Experimental investigation on the thermo-physical properties of Al2O3 nano particles suspended in car radiator coolant. *International Cvommunications in heat and mass transfer*.

Ethylene Glycol product Guide. (2018). Retrieved from global.biz: https://www.meglobal.biz/wp-content/uploads/2019/01/Monoethylene-Glycol-MEG-Technical-Product-Brochure-PDF.pdf?fbclid=IwAR2Db3EBFJfMoMzvZ8fvMbpB3eaPj_lJLSddXpHIQxknoYzAvxH1s0XLgn8

Evans, P. (2015, 03 29). *Properties of waterat atmospheric pressure*. Retrieved from The Engineering mindset .com.

Feynman, R. P. (1960). *There's plenty of room at the bottom.*

Furuya, M., & Kinoshita, I. (2002). Effects of polymer, surfactant, and salt additives to a coolant on the mitigation and the severity of vapor explosions. In *Experimental Thermal and Fluid Science, volume 26* (pp. 213-219). Elsevier.

Ghosh, C. K., Popuri, S. R., Mahesh, T. U., & Chattopadhyay, K. K. (2009). Preparation of nanocrystalline CuAlO 2 through sol–gel route. *Journal of sol-gel science and technology*, 75-81.

Hashemabadi, S. H., Peyghambarzadeh, S. M., Hoseini, S. M., & Jamnani, S. M. (2011). Experimental study of heat transfer enhancement using water/ethylene glycol based nanofluids as a new coolant for car radiators. *International Communications of Heat and Mass transfer*, 1283-1290.

History of Car Cooling System. (2018, November). Retrieved from ukessays.com.

Hollis, J. M., Lovas, F. J., Jewell, P. R., & Coudert, L. H. (2002). Interstellar Antifreeze: Ethylene Gylcol. *The Astrophysical Journal*.

Hwang, Y., Lee, J., Lee, C., Jung, Y., Cheong, S., & Lee, C. (2007). Stability and therml conductivity characteristics of nanofluids. 70-74.

Idik, N. A., YAzid, M. N., & Mamat, R. (2015). A review on the application of nanofluids in vehicle engine cooling system. *International Communications in Heat and Mass Transfer*, 85-90.

Instrumentation of a UV-Visible Spectrophotometer. (2023). Retrieved from jascoinic.com.

Jalvandi, J. (2016). Novel chemical and physical approaches for sustainable drug release from biodegradable electrospun nanofibres. *RMIT University PhD Thesis*.

Jangra, R. (2018). Analysis of Energy Storage from Exhaust of an Internal Combustion Engine. *ICADEMS*.

Jennifer, H. B., Marina, D. A., Anil, P. K., & E, S. M. (2007). Characterization of nanoparticles for therapeutics. *Nanomedicine*.

Jinsiwale, N., & Achawl, V. (2018). Heat transfer enhancement in automobile radiator using nanofluids. *55(2)*, 68-74.

Joseph A. Lima and George R. Otterman, e. (1989). *Manual on Selection and Use of Engine Coolants and Cooling System chemicals.* ASTM.

Judran, H. K., Al-Hasnawi, A., Al Zubaidi, N. F., Al-Maliko, W., Alobaid, F., & Epple, B. (2022). A High Thermal Conductivity of MgO-H2O Nanofluid Prepared by Two-Step Technique. *Applied sciences*, 2655.

Karagoz, Y. a. (2022). Effect of Al2O3 Addition to an internal combustion engine coolant on heat tranfer performance. *31*.

Ke-long, H., Liang-guo, Y., Su-qin, L., & Chao-jian, L. (2007). Preparation and formation mechanism of A1203 nanoparticles by reverse microemulsion. *Science press*, 633-637.

Khan, I., & Khalid Saeed, I. K. (2019). Nanoparticles: Properties, applications and toxicites. *Arabian Journal of Chemistry Volume 12, Issue 7*, 908-931.

Klein, J. (2007). Probing the interactions of proteins and nanoparticles. *Proceedings of the National Academy of Sciences of the United States of America*, 2029-2030.

Knorr, F., Sanchez, D. G., Schirmer, J., Gazdzicki, P., & Friedrich, K. A. (2019). Methanol as antifreeze agent for cold start of automotive polymer electroylter membrane fuel cells. *Applied Energy* , 1-10.

Kong, J., & Yu, S. (2007). Fourier Transform Infrared Spectroscopic Analysis of Protein Secondary Structres. *Acta Biochimica et Biophysica Sinica*, 549-559.

Kothvale, B., & Karad, V. (2014). Performance investigation of automobile radiator operated with Al2O3 base nanofluid. *IOSR Journal of Mechanical And Civil Engineering* .

Langelandsvik, G. (2017). *Optimization of Electrical Conductivity in Screw Extruded Wires.* Norwegian University of Science and Technology Master's Thesis.

Laurent, S., Forge, D., Port, M., Roch, A., Robic, C., Vander, E. L., & Muller, R. (2010). Magnetic Iron oxide nanoparticles: synthesis, stabilization, vectorization, physiochemical characterizations and biological applications. *Chem. Rev. 110*, 2574-2574.

Lin, P., Lin, S., Wang, P. C., & Sridhar, R. (2014). Techniques for physiochemical characterization of nanomaterials. *Biotechnology Advances*, 711-726.

Loos, M. (2015). Processing of Polymer Matrix Composites Containing CNTs. In *Carbon Nanotube Reinforced Composites* (pp. 171-188). William Andrew Applied Sciences Publishers.

Majhi, K. C., & Yadav, M. (2020). Types of nanomaterials. In Inamuddin, R. Boddula, M. Ahamed, & A. Asiri, *Green Sustainable Process for Chemical and Environmental Engineering and Science.* Elsevier.

Manuel, A. P. (2022, March 04). *Spectroscopic Techniques to Characterize Nanomaterials*. Retrieved from Lab Manager: https://www.labmanager.com/insights/spectroscopic-techniques-to-characterize-nanomaterials

Mayeen, A., Shaji, L. K., Nair, A. K., & Kalarikkal, N. (2018). Morphological Characterization of Nanomaterials. In *Characterization of Nanomaterials* (pp. 335-364). Woodhead publishing.

Minsta, H. A., Roy, G., Nguyen, C., & Doucet, D. (2009). New temperature dependent thermal conductivity data for water-based nanofluids. *International Journal of Thermal Sciences 48*, 363-371.

Mudalige, T., Qu, H., Haute, D. V., Ansar, S. M., Paredes, A., & Ingle, T. (2019). Characterization of Nanomaterials: Tools and Challenges. In *Nanomaterials for Food Applications* (pp. 313-353). Elsevier.

Mukherjee, S., & Paria, S. (2013). Preparation and stability of nanofluids-a review. *IOSR Journal of Mechanical and civil engineering*, 63-69.

Mukherjee, S., Halder, T., Ranjan, S., Bose, k., & Chakrabarty, S. (2021). Effects of SiO2 nanoparticles addition on performance of commercial engine coolant: Experimental investigation and empirical correlation. *231*.

Mutuku, W. N. (2016). Ethylene glycol (EG)-based nanofluids as a coolant for automotive radiator.

Nambeesan, K., Parthiban, R., Ram, K., Athul, U., Vivek, M., & Thirumalini, S. (2015). Experimental study of heat transfer enhancement in automobile radiator usinng al2O3/water-ethylene gylcol nanofluid coolants . *International journal of automotive and Mechanical Engineering*, 2857-2865.

Nanoparticle Characterization Techniques. (2022). Retrieved from nano composix: nanocomposix.com

Nguyen, C. T., Roy, G., Gauthier, C., & Galanis, N. (2007). *Applied thermal engineering* , 1501-1506.

Nutan, S. S., & Dhoble, S. J. (2021). Role of rare-earth ions for energy-saving LED lighting devices. In *Energy Materials* (pp. 407-444). Elsevier.

Pak, B., & Cho, I. (1998). Hydrodyanamic and heat transfer study of dispersed fluif with sub - micron metallic oxid particles. 151-170.

Palani, S., Irudhayarai, R., Vigneshwaran, M., & Selvam, M. M. (2016). Study of Cooling System in I.C. Enginer Improving Performance with Reduction of cost. *Indian Journal of Science and technology*.

Pantzali, M. N., Kanaris, A., Antoniadis, K., Mouza, A. A., & Paras, S. V. (2009). Effect of nanofluids on the performance of a miniature plate heat exchanger with modulated surface. *International Journal of Heat Fluid Flow*.

Pathade, V., Satpute, S., Lajurkar, M., Pancheshwar, G., Karluke, T., & Singitvar, N. (2017). DESIGN AND ANALYSIS OF CAR RADIATOR BY FINITE ELEMENT METHOD. *IJARIIE*, 2395-4396.

Prof. Meshram, A. D., Prof. Naik, A., & Prof. Sonparate, A. (2015). Heat Transfer enhancement of Effect of Thermal Conductivity by Nanofluids. *International Research Journal of Engineeering and technology, 2*(09).

Rathodiya, B., & Vishnoi, S. (2017). PREPARATION METHODS FOR NANOFLUIDS AND THERE STABILITY. 2320-2882.

Rose, J. (2015). Characterization of Nanomaterials in Complex Environmental and Biological Media. In *Frontiers of Nanoscience* (pp. 217-243). Elsevier.

RUIAN SHERROCK. (2021). Retrieved from Sheradiatir: https://www.sheradiatortank.com

Sahoo, A. R. (2015). *Synthesis and characterization of a-Al2O3 by solgel method process and development of Zn-Al203 compositesby Powder metallurgy Route.* Odisha.

Sandhya, M., Ramasamy, D., Sudhakar, K., Kadirgama, K., & Harun, W. (2021). Ultrasonication an intensifying tool for preparation of stable nanofluids and study the time influence on distinct properties of graphene nanofluids - A systematic overview. In *Ultrasonics Sonochemistry.* Elsevier.

Saripella, S., Yu, W., Routbort, J., France, D., & Rizwan-Uddin. (2007). Effects of nanofluid coolant in a class 8 truck engine. *SAE Technical Paper*.

Sarker, S. D., & Nahar, L. (2022). Characterization of nanoparticles. In *Advances in Nanotechnology-Based Drug Delivery Systems* (pp. 45-82). Elsevier.

Septiadi, W. N., Trisnadewi, I. A., Putra, N., & Setyawan, I. (2018). Synthesis of hybrid nanofluid with two-step method. *In E3S Web of Conferences EDP Sciences*.

Shehata, F., Fathy, A., Abdelhameed, M., & Moustafa, S. (2009). Preparation and properties of Al2O3 Nanoparticle reinforced copper matrix compositesby in situ processing. *Materials and Design*, 2756-2762.

Sivakumar, M., Tang, S., & Tan, K. (2014). Cavitation technology - a greener processing technique for the generation of pharmaceutical nanoemulsions. *Ultrasonics Sonochemistry*, 2069-2083.

Smith, K. M., & Holroyd, P. (2013). Heat. In *Engineering Principles for Electrical Technicians.* Elsevier.

Stefl, B., & George, K. (2000). Antifreezes and Deicing Fluid. *Kirk-Othmer Encyclopedia of Chemical Technology*.

Studentlesson. (2020, September 7). Retrieved from studentlesson.com: https://studentlesson.com/radiator-definition-functions-parts-diagram-working/

Sudarmadji, S., Soeparman, S., Wahyudi, S., & Hamidy, N. (2014). Effects of cooling process of Al2O3- water nanofluid on convective heat transfer. 155-160.

Suresh, S., Venkitaraj, K. P., Selvakumar, P., & Chandrasekar, M. (2011). Synthesis of Al2O3Cu/water hybrid nanofluids using two step method and its thermo physical properties. *Colloids and Surfaces A: Physicochemical and Engineering Aspects*, 41-48.

Tabesh, S., Davar, F., & Loghman-Estarki, M. R. (2018). Preparation of γ-〖Al〗_2 O_3 nanoparticles using modified sol-gel method and its use for the adsorption of lead and cadmium ions. *Journal of Alloys and Compounds*, 441-449.

Tata Motors Product. (n.d.). Retrieved from Tata Tiago specification: cars.tatamotors.com/cars/tiago/specifications

The Engineerig ToolBox. (2001). Retrieved from www.EngineeringToolBox.com.

The Versatile Fluid That Changed The World. (2018). Retrieved from sensibledriver.com: https://sensibledriver.com/article/the-versatile-fluid-that-changed-the-world#:~:text=The%20fascinating%20history%20of%20antifreeze,pump%20and%20transmit%20through%20lines.

Types of Cooling System in Car Engine: Components & Function. (2021). Retrieved from Engineering Learn: engineering learn.com

UV-Vis Spectrophotometer. (2020). Retrieved from smac gig world: smacgigworld.com

Vaijha, R., Das, D., & Namburu, P. (2010). Numerical study of fluid dynamic and heat transfer performance of Al2O3 and CuO nanofluids in the flat tubes of a radiator. *International Journal of Heat and Fluid Flow*.

Vajjha, R., Das, D., & Ray, D. R. (2015). Development of new correlations for the Nusselt number and the friction factor under turbulent flow of nanofluids in flat tubes. *International Journal of Heat Mass Transfer vol. 80*, 253-367.

Vasu, V., Ramakrishna, K., & S. Kumar, A. (2008). *International Journal of Nano Technologies Applicaion*.

Venkatesan, S. &. (2015). Improving the heat removal rate using nano particle mixed coolant in radiator. *Journal of Chemical and Pharmaceutical Sciences*, 351-354.

Vithayasai, S., Kiatsiriroat, T., & Nuntaphan, A. (2006). Effect of electric field on heat transfer performance of automobile radiator at low frontal air velocity. *Applied Thermal Engineering*, 2073-2078.

Wen, D., & Ding, Y. (2004). Experimental investigation into convective heat transfer of nanofluids at the entrance region under laminar flow conditions. *International Journal of Heat Mass Transfer 47*, 5181-8188.

Xie, H., Wang, J., Xi, T., Liu, Y., & Ai, F. (2002). Thermal conductivity enhancement of suspensions containing nanosize alumina particles. *Journal of Applied Physics*.

Xu, L., Liang, H. W., Yang, Y., & Yu, S. H. (2018). Stability and Reactivity: Positive and Negative aspects for Nanoparticle Processing.

Xuan, Y., & Li, Q. (2000). Heat transfer enhancement of Nanofluids. *International Journal of Heat and Fluid Flow*, 58-64.

Yang, K. Z., Pramanik, A., Basak, A., Dong, Y., Prakash, C., Shankar, S., . . . Vatin, N. I. (2023). Application of coolants during tool-based machining- A review. *Ain Shams Engineering Journal*.

Yilmaz, C. N., Karasulu, H. Y., & Yilmaz, O. (2019). Nanoscaled Dispersed Systems Used in Drug-Delivery Applications. In *Polymeric Nanomaterials in Nanotherapeutics* (pp. 437-468). Elsevier.

Zaki, T., kabel, K., & Hassan, H. (2012). Preparation of high pure a-Al2O3 nanoparticles at low temperatures using Pechini method. *Ceramics International*, 2021-2026.

Zhang, K. J., Wang, D., Hou, J., Jiang, H., Li, J., Liu, G., & Zhang, X. (2007). Characteristic and experiment study of HDD engine coolants. *Neiranji Gongcheng/ China International Comubistion Engine Engineering*, 75-78.

Zhang, Y. a., Xiaoli, L. a., G.-D.and Huang, L.-W., & X.-J and Liao, S.-P. (2006). Research of loader cooling system overheat prob;em. 1183-1186.

Zhu, H. T., Lin, Y. S., & Yin, Y. S. (2004). A novel one-step chemical method for preparation of copper nanofluids. *Journal of Colloid and Interface Science, vol. 277*, 100-103.

APPENDIX A: UV-Vis spectrophotometer data

wavelength	hv	hvfr
200	6.1985	0.174
201	6.167661692	0.157
202	6.137128713	0.146
203	6.106896552	0.121
204	6.076960784	0.116
205	6.047317073	0.107
206	6.017961165	0.102
207	5.988888889	0.098
208	5.960096154	0.094
209	5.931578947	0.087
210	5.903333333	0.09
211	5.87535545	0.094
212	5.847641509	0.098
213	5.820187793	0.108
214	5.792990654	0.111
215	5.766046512	0.122
216	5.739351852	0.132
217	5.712903226	0.145
218	5.686697248	0.171
219	5.660730594	0.179
220	5.635	0.197
221	5.609502262	0.203
222	5.584234234	0.206
223	5.559192825	0.211
224	5.534375	0.208
225	5.509777778	0.205
226	5.48539823	0.208
227	5.46123348	0.21
228	5.437280702	0.208
229	5.413537118	0.203
230	5.39	0.203
231	5.366666667	0.203
232	5.343534483	0.203
233	5.320600858	0.199
234	5.297863248	0.202
235	5.275319149	0.197
236	5.252966102	0.198
237	5.230801688	0.195
238	5.208823529	0.196
239	5.187029289	0.197
240	5.165416667	0.196

wavelength	hv	hvfr
241	5.143983402	0.196
242	5.122727273	0.195
243	5.101646091	0.198
244	5.080737705	0.198
245	5.06	0.2
246	5.039430894	0.202
247	5.01902834	0.205
248	4.998790323	0.204
249	4.978714859	0.206
250	4.9588	0.203
251	4.939043825	0.209
252	4.919444444	0.208
253	4.9	0.213
254	4.880708661	0.209
255	4.861568627	0.208
256	4.842578125	0.205
257	4.823735409	0.205
258	4.80503876	0.209
259	4.786486486	0.21
260	4.768076923	0.21
261	4.749808429	0.208
262	4.731679389	0.206
263	4.713688213	0.208
264	4.695833333	0.207
265	4.678113208	0.208
266	4.660526316	0.208
267	4.643071161	0.211
268	4.625746269	0.207
269	4.608550186	0.21
270	4.591481481	0.208
271	4.574538745	0.206
272	4.557720588	0.209
273	4.541025641	0.205
274	4.524452555	0.203
275	4.508	0.202
276	4.491666667	0.201
277	4.475451264	0.197
278	4.459352518	0.194
279	4.443369176	0.193
280	4.4275	0.19
281	4.411743772	0.192

wavelength	hv	hvfr
282	4.396099291	0.186
283	4.380565371	0.188
284	4.365140845	0.182
285	4.349824561	0.18
286	4.334615385	0.176
287	4.319512195	0.176
288	4.304513889	0.174
289	4.289619377	0.171
290	4.274827586	0.168
291	4.260137457	0.167
292	4.245547945	0.162
293	4.23105802	0.158
294	4.216666667	0.159
295	4.202372881	0.156
296	4.188175676	0.153
297	4.174074074	0.152
298	4.160067114	0.15
299	4.146153846	0.146
300	4.132333333	0.145
301	4.118604651	0.141
302	4.104966887	0.142
303	4.091419142	0.139
304	4.077960526	0.137
305	4.064590164	0.133
306	4.05130719	0.133
307	4.038110749	0.131
308	4.025	0.127
309	4.01197411	0.125
310	3.999032258	0.122
311	3.986173633	0.12
312	3.973397436	0.119
313	3.960702875	0.115
314	3.948089172	0.116
315	3.935555556	0.111
316	3.923101266	0.11
317	3.910725552	0.109
318	3.898427673	0.106
319	3.886206897	0.104
320	3.8740625	0.101
321	3.861993769	0.098
322	3.85	0.096

wavelength	hv	hvfr
323	3.838080495	0.095
324	3.826234568	0.092
325	3.814461538	0.091
326	3.802760736	0.088
327	3.791131498	0.086
328	3.779573171	0.083
329	3.768085106	0.082
330	3.756666667	0.078
331	3.745317221	0.077
332	3.734036145	0.076
333	3.722822823	0.073
334	3.711676647	0.071
335	3.700597015	0.07
336	3.689583333	0.068
337	3.678635015	0.067
338	3.667751479	0.064
339	3.656932153	0.062
340	3.646176471	0.061
341	3.635483871	0.059
342	3.624853801	0.056
343	3.614285714	0.055
344	3.60377907	0.054
345	3.593333333	0.052
346	3.582947977	0.05
347	3.572622478	0.049
348	3.562356322	0.047
349	3.552148997	0.045
350	3.542	0.044
351	3.531908832	0.042
352	3.521875	0.04
353	3.511898017	0.039
354	3.501977401	0.038
355	3.492112676	0.036
356	3.482303371	0.035
357	3.47254902	0.034
358	3.462849162	0.032
359	3.453203343	0.031
360	3.443611111	0.03
361	3.434072022	0.029
362	3.424585635	0.028
363	3.415151515	0.026

wavelength	hv	hvfr
364	3.405769231	0.025
365	3.396438356	0.025
366	3.38715847	0.023
367	3.377929155	0.023
368	3.36875	0.022
369	3.359620596	0.021
370	3.350540541	0.021
371	3.341509434	0.02
372	3.332526882	0.02
373	3.323592493	0.018
374	3.314705882	0.018
375	3.305866667	0.016
376	3.297074468	0.016
377	3.288328912	0.015
378	3.27962963	0.015
379	3.270976253	0.015
380	3.262368421	0.014
381	3.253805774	0.014
382	3.245287958	0.013
383	3.236814621	0.012
384	3.228385417	0.012
385	3.22	0.011
386	3.211658031	0.011
387	3.203359173	0.01
388	3.195103093	0.01
389	3.18688946	0.009
390	3.178717949	0.009
391	3.170588235	0.009
392	3.1625	0.009
393	3.154452926	0.008
394	3.146446701	0.008
395	3.138481013	0.007
396	3.130555556	0.007
397	3.122670025	0.007
398	3.114824121	0.006
399	3.107017544	0.006
400	3.09925	0.006
401	3.091521197	0.006
402	3.083830846	0.006
403	3.07617866	0.005
404	3.068564356	0.005

wavelength	hv	hvfr
405	3.060987654	0.005
406	3.053448276	0.005
407	3.045945946	0.005
408	3.038480392	0.004
409	3.031051345	0.004
410	3.023658537	0.004
411	3.016301703	0.004
412	3.008980583	0.004
413	3.001694915	0.004
414	2.994444444	0.004
415	2.987228916	0.004
416	2.980048077	0.003
417	2.972901679	0.003
418	2.965789474	0.003
419	2.958711217	0.003
420	2.951666667	0.003
421	2.944655582	0.003
422	2.937677725	0.003
423	2.930732861	0.003
424	2.923820755	0.003
425	2.916941176	0.003
426	2.910093897	0.003
427	2.903278689	0.003
428	2.896495327	0.002
429	2.88974359	0.002
430	2.883023256	0.002
431	2.876334107	0.002
432	2.869675926	0.002
433	2.863048499	0.002
434	2.856451613	0.002
435	2.849885057	0.002
436	2.843348624	0.002
437	2.836842105	0.002
438	2.830365297	0.002
439	2.823917995	0.002
440	2.8175	0.002
441	2.811111111	0.002
442	2.804751131	0.002
443	2.798419865	0.002
444	2.792117117	0.002
445	2.785842697	0.002

wavelength	hv	hvfr
446	2.779596413	0.002
447	2.773378076	0.002
448	2.7671875	0.002
449	2.761024499	0.002
450	2.754888889	0.002
451	2.748780488	0.002
452	2.742699115	0.002
453	2.736644592	0.002
454	2.73061674	0.002
455	2.724615385	0.002
456	2.718640351	0.002
457	2.712691466	0.002
458	2.706768559	0.002
459	2.70087146	0.002
460	2.695	0.002
461	2.689154013	0.001
462	2.683333333	0.001
463	2.677537797	0.001
464	2.671767241	0.001
465	2.666021505	0.001
466	2.660300429	0.001
467	2.654603854	0.001
468	2.648931624	0.001
469	2.643283582	0.001
470	2.637659574	0.001
471	2.632059448	0.001
472	2.626483051	0.001
473	2.620930233	0.001
474	2.615400844	0.001
475	2.609894737	0.001
476	2.604411765	0.001
477	2.598951782	0.001
478	2.593514644	0.001
479	2.588100209	0.001
480	2.582708333	0.001
481	2.577338877	0.001
482	2.571991701	0.001
483	2.566666667	0.001
484	2.561363636	0.001
485	2.556082474	0.001
486	2.550823045	0.001

wavelength	hv	hvfr
487	2.545585216	0.001
488	2.540368852	0.001
489	2.535173824	0.001
490	2.53	0.001
491	2.524847251	0.001
492	2.519715447	0.001
493	2.514604462	0.001
494	2.50951417	0.001
495	2.504444444	0.001
496	2.499395161	0.001
497	2.494366197	0.001
498	2.48935743	0.001
499	2.484368737	0.001
500	2.4794	0.001
501	2.474451098	0.001
502	2.469521912	0.001
503	2.464612326	0.001
504	2.459722222	0.001
505	2.454851485	0.001
506	2.45	0.001
507	2.445167653	0.001
508	2.440354331	0.001
509	2.435559921	0.001
510	2.430784314	0.001
511	2.426027397	0.001
512	2.421289063	0.001
513	2.416569201	0.001
514	2.411867704	0.001
515	2.407184466	0.001
516	2.40251938	0.001
517	2.39787234	0.001
518	2.393243243	0.001
519	2.388631985	0.001
520	2.384038462	0.001
521	2.379462572	0.001
522	2.374904215	0.001
523	2.370363289	0.001
524	2.365839695	0.001
525	2.361333333	0.001
526	2.356844106	0.001
527	2.352371917	0.001

wavelength	hv	hvfr
528	2.347916667	0.001
529	2.343478261	0.001
530	2.339056604	0.001
531	2.334651601	0.001
532	2.330263158	0.001
533	2.325891182	0.001
534	2.321535581	0.001
535	2.317196262	0.001
536	2.312873134	0.001
537	2.308566108	0.001
538	2.304275093	0.001
539	2.3	0.001
540	2.295740741	0.001
541	2.291497227	0.001
542	2.287269373	0.001
543	2.28305709	0.001
544	2.278860294	0.001
545	2.274678899	0.001
546	2.270512821	0.001
547	2.266361974	0.001
548	2.262226277	0.001
549	2.258105647	0.001
550	2.254	0.001
551	2.249909256	0.001
552	2.245833333	0.001
553	2.241772152	0.001
554	2.237725632	0.001
555	2.233693694	0.001
556	2.229676259	0.001
557	2.22567325	0.001
558	2.221684588	0.001
559	2.217710197	0.001
560	2.21375	0.001
561	2.209803922	0.001
562	2.205871886	0.001
563	2.201953819	0.001
564	2.198049645	0.001
565	2.194159292	0.001
566	2.190282686	0.001
567	2.186419753	0.001
568	2.182570423	0.001

wavelength	hv	hvfr
569	2.178734622	0.001
570	2.174912281	0.001
571	2.171103327	0.001
572	2.167307692	0.001
573	2.163525305	0.001
574	2.159756098	0.001
575	2.156	0.001
576	2.152256944	0.001
577	2.148526863	0.001
578	2.144809689	0.001
579	2.141105354	0.001
580	2.137413793	0.001
581	2.13373494	0.001
582	2.130068729	0.001
583	2.126415094	0.001
584	2.122773973	0.001
585	2.119145299	0.001
586	2.11552901	0.001
587	2.111925043	0.001
588	2.108333333	0.001
589	2.10475382	0.001
590	2.101186441	0.001
591	2.097631134	0.001
592	2.094087838	0.001
593	2.090556492	0.001
594	2.087037037	0.001
595	2.083529412	0.001
596	2.080033557	0.001
597	2.076549414	0.001
598	2.073076923	0.001
599	2.069616027	0.001
600	2.066166667	0.001
601	2.062728785	0.001
602	2.059302326	0.001
603	2.055887231	0.001
604	2.052483444	0.001
605	2.049090909	0.001
606	2.045709571	0.001
607	2.042339374	0.001
608	2.038980263	0.001
609	2.035632184	0.001

wavelength	hv	hvfr
610	2.032295082	0.001
611	2.028968903	0.001
612	2.025653595	0.001
613	2.022349103	0.001
614	2.019055375	0.001
615	2.015772358	0.001
616	2.0125	0.001
617	2.00923825	0.001
618	2.005987055	0.001
619	2.002746365	0.001
620	1.999516129	0.001
621	1.996296296	0.001
622	1.993086817	0.001
623	1.98988764	0.001
624	1.986698718	0.001
625	1.98352	0.001
626	1.980351438	0.001
627	1.977192982	0.001
628	1.974044586	0.001
629	1.9709062	0.001
630	1.967777778	0.001
631	1.964659271	0.001
632	1.961550633	0.001
633	1.958451817	0.001
634	1.955362776	0.001
635	1.952283465	0.001
636	1.949213836	0.001
637	1.946153846	0.001
638	1.943103448	0.001
639	1.940062598	0.001
640	1.93703125	0.001
641	1.93400936	0.001
642	1.930996885	0.001
643	1.927993779	0.001
644	1.925	0.001
645	1.922015504	0.001
646	1.919040248	0.001
647	1.916074189	0.001
648	1.913117284	0.001
649	1.910169492	0.001
650	1.907230769	0.001

wavelength	hv	hvfr
651	1.904301075	0.001
652	1.901380368	0.001
653	1.898468606	0.001
654	1.895565749	0.001
655	1.892671756	0.001
656	1.889786585	0.001
657	1.886910198	0.001
658	1.884042553	0.001
659	1.881183612	0.001
660	1.878333333	0.001
661	1.875491679	0.001
662	1.87265861	0.001
663	1.869834087	0.001
664	1.867018072	0.001
665	1.864210526	0.001
666	1.861411411	0.001
667	1.85862069	0.001
668	1.855838323	0.001
669	1.853064275	0.001
670	1.850298507	0.001
671	1.847540984	0.001
672	1.844791667	0.001
673	1.84205052	0.001
674	1.839317507	0.001
675	1.836592593	0.001
676	1.83387574	0.001
677	1.831166913	0.001
678	1.828466077	0.001
679	1.825773196	0.001
680	1.823088235	0.001
681	1.82041116	0.001
682	1.817741935	0.001
683	1.815080527	0.001
684	1.812426901	0.001
685	1.809781022	0.001
686	1.807142857	0.001
687	1.804512373	0.001
688	1.801889535	0.001
689	1.799274311	0.001
690	1.796666667	0.001